Electronic Supplementary Material (ESI) for Dalton Transactions.
This journal is © The Royal Society of Chemistry 2016

Oxygen activation and catalytic aerobic oxidation by Mo(IV)/(VI) complexes with functionalized iminophenolate ligands

Niklas Zwettler,[†] *Martina E.Judmaier,*[†] *Lara Strohmeier,*[†] *Ferdinand Belaj*[†] *and Nadia C. Mösch-Zanetti*[†,*]

[†] Institute of Chemistry, Inorganic Chemistry, University of Graz, Schubertstrasse 1, 8010 Graz, Austria

Supporting Information

^{1}H, ^{13}C and HSQC NMR spectra.. 4
Figure S1. Proton NMR spectrum of complex **1** [$MoO_2(L1)_2$] in C_6D_6. 4
Figure S2. Carbon NMR spectrum of complex **1** [$MoO_2(L1)_2$] in C_6D_6. 4
Figure S3. HSQC NMR spectrum of complex **1** [$MoO_2(L1)_2$] in C_6D_6. 5
Figure S5. HSQC NMR spectrum of complex **2** [$MoO_2(L2)_2$] in C_6D_6. 6
Figure S6. VT NMR spectrum of complex **2** [$MoO_2(L2)_2$] in C_6D_6 6
Figure S7. Aromatic region of ^{1}H NMR spectra of complex **2** [$MoO_2(L2)_2$] in C_6D_6 (top), CD_2Cl_2 (middle) and CD_3CN (bottom) 7
Figure S8. Proton NMR spectrum of complex **3** [MoO_2(acac)(L2)] in C_6D_6.......................... 7
Figure S9. Carbon NMR spectrum of complex **3** [MoO_2(acac)(L2)] in C_6D_6. 8
Figure S10. HSQC NMR spectrum of complex **3** [MoO_2(acac)(L2)] in C_6D_6........................ 8
Figure S11. Proton NMR spectrum of the isomeric mixture of complex **4** [$MoO_2(PMe_3)(L1)_2$] in C_6D_6. 9
Figure S12. Carbon NMR spectrum of the isomeric mixture of complex **4** [$MoO_2(PMe_3)(L1)_2$] in C_6D_6. 9
Figure S13. Phosphorus NMR spectrum of the isomeric mixture of complex **4** [$MoO_2(PMe_3)(L1)_2$] in C6D6... 10
Figure S14. HSQC NMR spectrum of the isomeric mixture of complex **4** [$MoO_2(PMe_3)(L1)_2$] in C_6D_6. 10
Figure S15. Proton NMR spectrum of the isomeric mixture of complex **5** [$MoO_2(PMe_3)(L2)_2$] in C_6D_6. 11
Figure S16. Proton NMR spectrum of the pure O,O isomer of of complex **5** [$MoO_2(PMe_3)(L2)_2$] in C_6D_6, obtained via recrystallization from MeCN.............................. 11
Figure S17. Carbon NMR spectrum of the isomeric mixture of complex **5** [$MoO_2(PMe_3)(L2)_2$] in C_6D_6... 12
Figure S18. Phosphorus NMR spectrum of the isomeric mixture of complex **5** [$MoO_2(PMe_3)(L2)_2$] in C_6D_6. 12
Figure S19. HSQC NMR spectrum of the isomeric mixture of complex **5** [$MoO_2(PMe_3)(L2)_2$] in C_6D_6... 13
Figure S20. Proton NMR spectrum of complex **6** {[$MoO(L1)_2]_2(\mu$-O)} in C_6D_6.................. 13
Figure S21. Carbon NMR spectrum of complex **6** {[$MoO(L1)_2]_2(\mu$-O)} in C_6D_6. 14
Figure S22. HSQC NMR spectrum of complex **6** {[$MoO(L1)_2]_2(\mu$-O)} in C_6D_6. 14
Figure S23. Proton NMR spectrum of complex **7** {[$MoO(L2)_2]_2(\mu$-O)} in C_6D_6.................. 15
Figure S24. Carbon NMR spectrum of complex **7** {[$MoO(L2)_2]_2(\mu$-O)} in C_6D_6. 15
Figure S25. HSQC NMR spectrum of complex **7** {[$MoO(L2)_2]_2(\mu$-O)} in C_6D_6. 16
Figure S26. Proton NMR spectrum of complex **8** [$MoO(O_2)(L1)_2$] in C6D6. 16
Figure S27. Carbon NMR spectrum of complex **8** [$MoO(O_2)(L1)_2$] in C_6D_6. 17
Figure S28. HSQC NMR spectrum of complex **8** [$MoO(O_2)(L1)_2$] in C_6D_6. 17
Figure S29. Proton NMR spectrum of the isomeric mixture of complex **9** [$MoO(O_2)(L2)_2$] in C_6D_6 with the O,O isomer assigned... 18
Figure S30. Proton NMR spectrum of the O,O isomer of complex **9** [$MoO(O_2)(L2)_2$] in C_6D_6 obtained via recrystallization from MeCN and immediate measurement. 18
Figure S31. Aromatic region of the ^{1}H NMR spectra of the initial isomeric mixture and dissolved single crystals of **9** [$MoO(O_2)(L2)_2$] after t=0.25 h and t=24 h in C_6D_6 showing the isomeric equilibration... 19
Figure S32. HSQC NMR spectrum of the isomeric mixture of complex **9** [$MoO(O_2)(L2)_2$] in C_6D_6 with the major isomer assigned. 19
Figure S33. Proton NMR resonances of the catalytic aerobic oxidation of PMe_3 using 1 mol% of **1**.. 20
Figure S34. Phosphorus NMR resonances of the catalytic aerobic oxidation of PMe_3 using 1 mol% of **1**.. 20
Figure S35. Proton NMR resonances of the catalytic aerobic oxidation of PPh_3 using 1 mol% of **1** 21

Figure S36. Phosphorus NMR resonances of the catalytic aerobic oxidation of PPh_3 using 1 mol% of **1** 21
Figure S37. Proton NMR resonances of the catalytic aerobic oxidation of PMe_3 using 1 mol% of **2** 22
Figure S38. Phosphorus NMR resonances of the catalytic aerobic oxidation of PMe_3 using 1 mol% of **2** 22
Figure S39. Proton NMR resonances of the catalytic aerobic oxidation of PPh_3 using 1 mol% of **2** 23
Figure S40. Phosphorus NMR resonances of the catalytic aerobic oxidation of PPh_3 using 1 mol% of **2** 23
Figure S41. Proton NMR resonances of the catalytic aerobic oxidation of PPh_3 using 1 mol% of **6** 24
Figure S42. Phosphorus NMR resonances of the catalytic aerobic oxidation of PPh_3 using 1 mol% of **6** 24
Figure S43. Proton NMR resonances of the catalytic aerobic oxidation of PPh_3 using 1 mol% of **7** 25
Figure S44. Phosphorus NMR resonances of the catalytic aerobic oxidation of PPh_3 using 1 mol% of **7** 25
Figure S45. Selected Proton NMR resonances of a reaction of **9** $[MoO(O_2)(L2)_2]$ with 2 equiv of PMe_3 after t=6h showing a mixture of **5** 26
Table S1. Selected crystallographic data and structure refinement for **1-3**, **5**, **6**, **8** and **9**. 27
Structure determination of 1. 28
Figure S46. Stereoscopic ORTEP[2] plot of **1** 29
Table S2. Additional crystal data and structure refinement for **1**. 29
Table S3. Selected bond lengths [Å] and angles [°] for **1**. 30
Structure determination of 2. 31
Figure S47. Stereoscopic ORTEP[2] plot of of molecule **A** of **2** 32
Figure S48. Stereoscopic ORTEP[2] plot of of molecule **B** of **2**. 32
Table S4. Additional crystal data and structure refinement for **2**. 33
Table S5. Selected bond lengths [Å] and angles [°] for **2**. 33
Structure determination of 3. 35
Figure S49. Stereoscopic ORTEP[2] plot of one of the four complexes of the asymmetric unit of **3** 36
Figure S50. ORTEP[2] plot of the four complexes of the asymmetric unit of **3**. 36
Table S6. Additional crystal data and structure refinement for **3**. 36
Table S7. Selected bond lengths [Å] and angles [°] for **2**. 37
Structure determination of 5. 39
Figure S51. Stereoscopic ORTEP[2] plot of **5** 40
Table S8. Additional crystal data and structure refinement for **5**. 40
Table S9. Selected bond lengths [Å] and angles [°] for **5**. 41
Crystal structure determination of 6. 42
Figure S52. Stereoscopic ORTEP[2] plot of **6** 43
Table S10. Additional crystal data and structure refinement for **6**. 43
Table S11. Selected bond lengths [Å] and angles [°] for **6**. 44
Crystal structure determination of 8. 45
Figure S53. Stereoscopic ORTEP[2] plot of **8** 46
Table S12. Additional crystal data and structure refinement for **8**. 46
Table S13. Selected bond lengths [Å] and angles [°] for **8**. 47
Crystal structure determination of 9. 48
Figure S54. Stereoscopic ORTEP[2] plot of **9** 49
Table S14. Additional crystal data and structure refinement for **9**. 49
Table S15. Selected bond lengths [Å] and angles [°] for **9**. 50
References 50

^1H, ^{13}C and HSQC NMR spectra

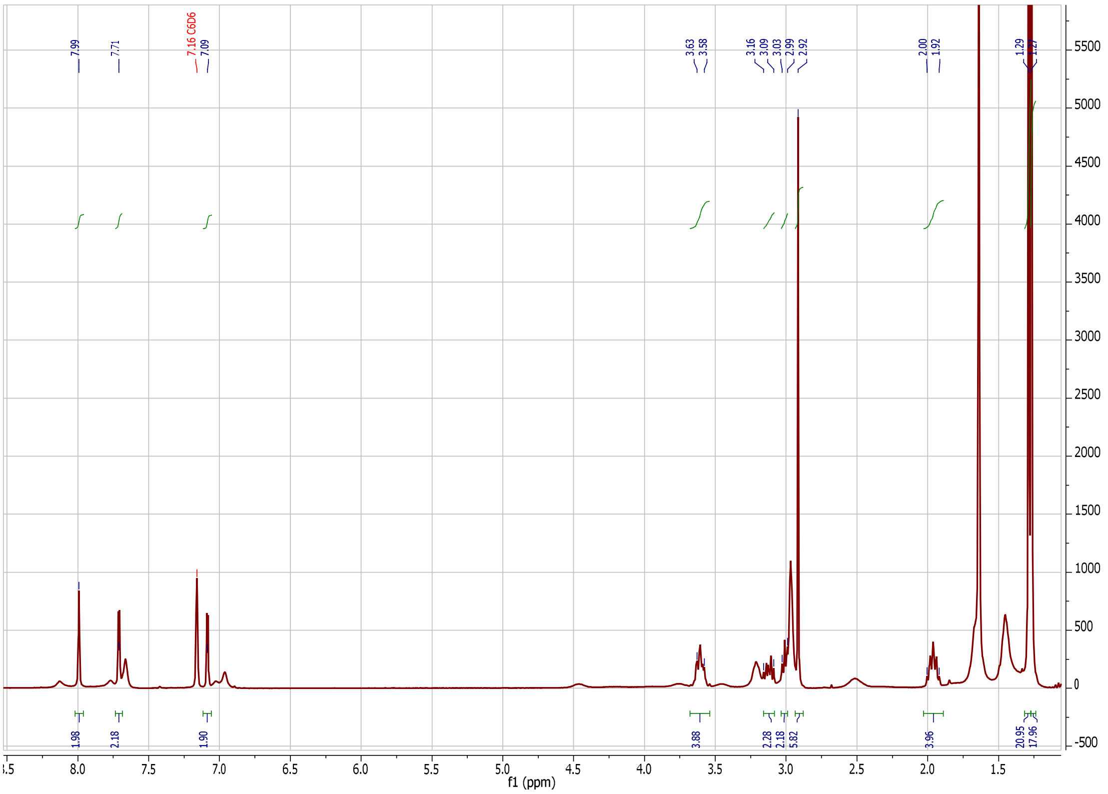

Figure S1. Proton NMR spectrum of complex **1** [$MoO_2(L1)_2$] in C_6D_6. The additional broad peaks, referring to a second isomer in solution, did not allow for meaningful assignment.

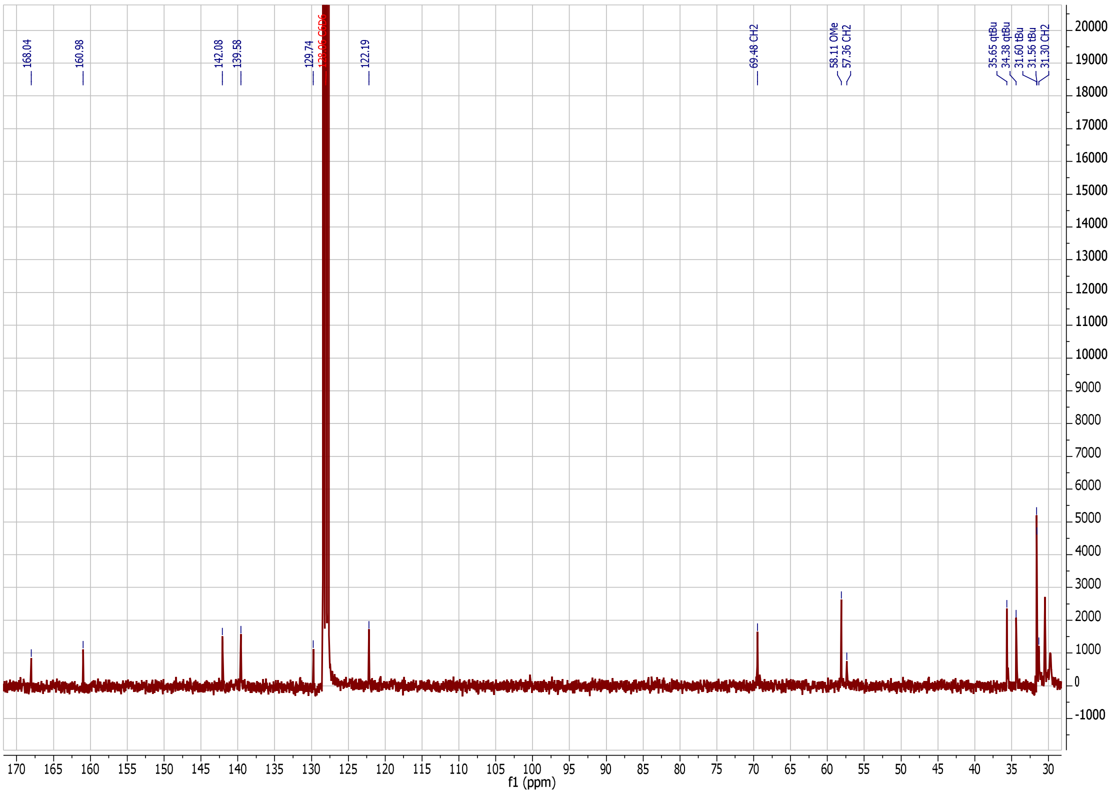

Figure S2. Carbon NMR spectrum of complex **1** [$MoO_2(L1)_2$] in C_6D_6.

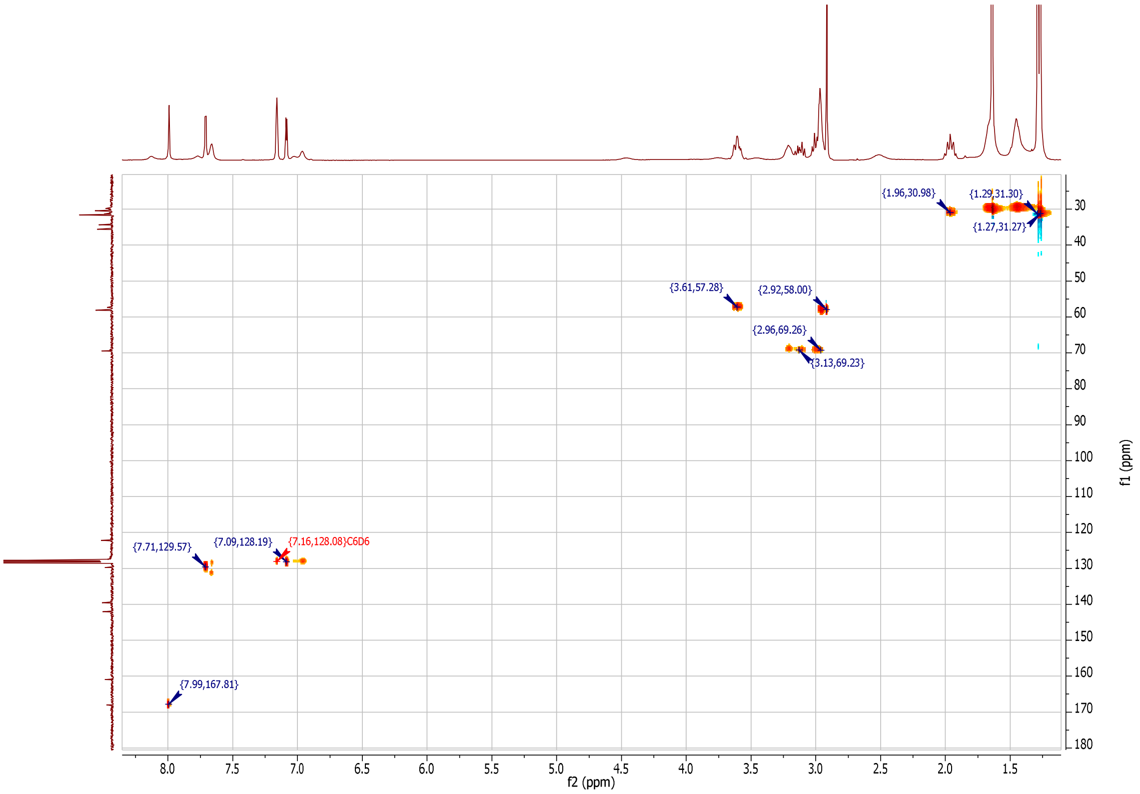

Figure S3. HSQC NMR spectrum of complex **1** [MoO$_2$(L1)$_2$] in C$_6$D$_6$.

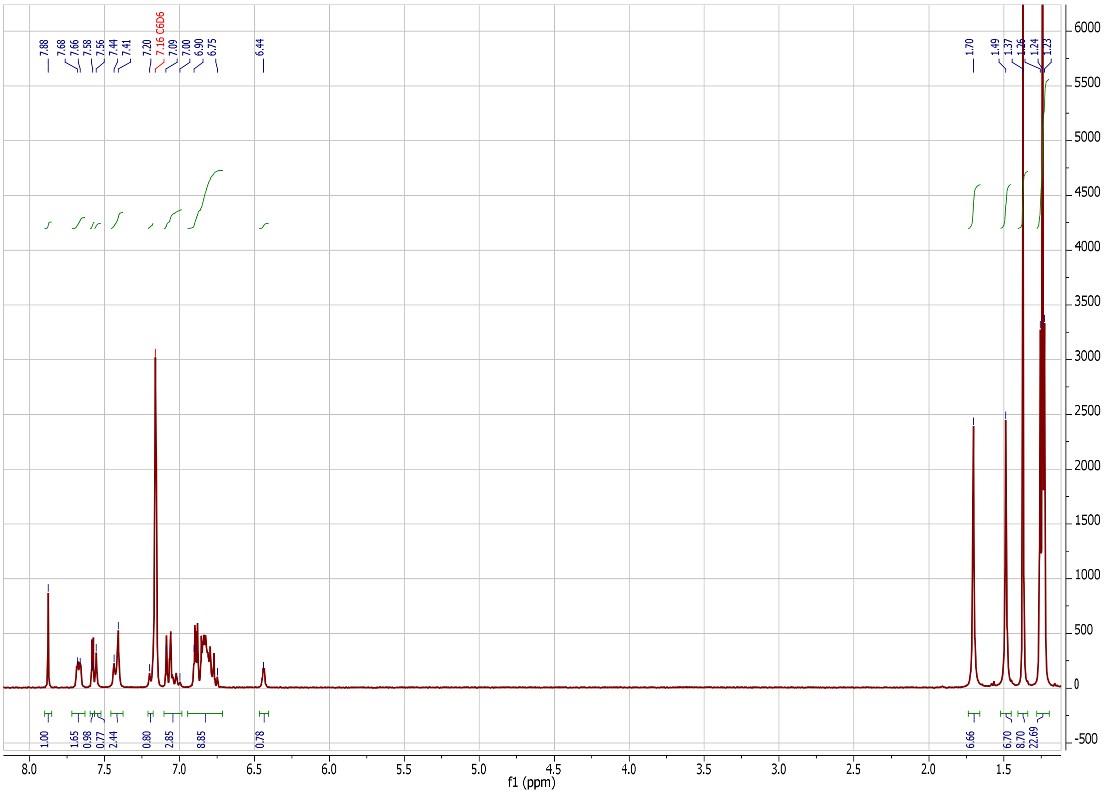

Figure S4. Proton NMR spectrum of complex **2** [MoO$_2$(L2)$_2$] in C$_6$D$_6$. The resonances were assigned to the two isomers with respect to their intensity.

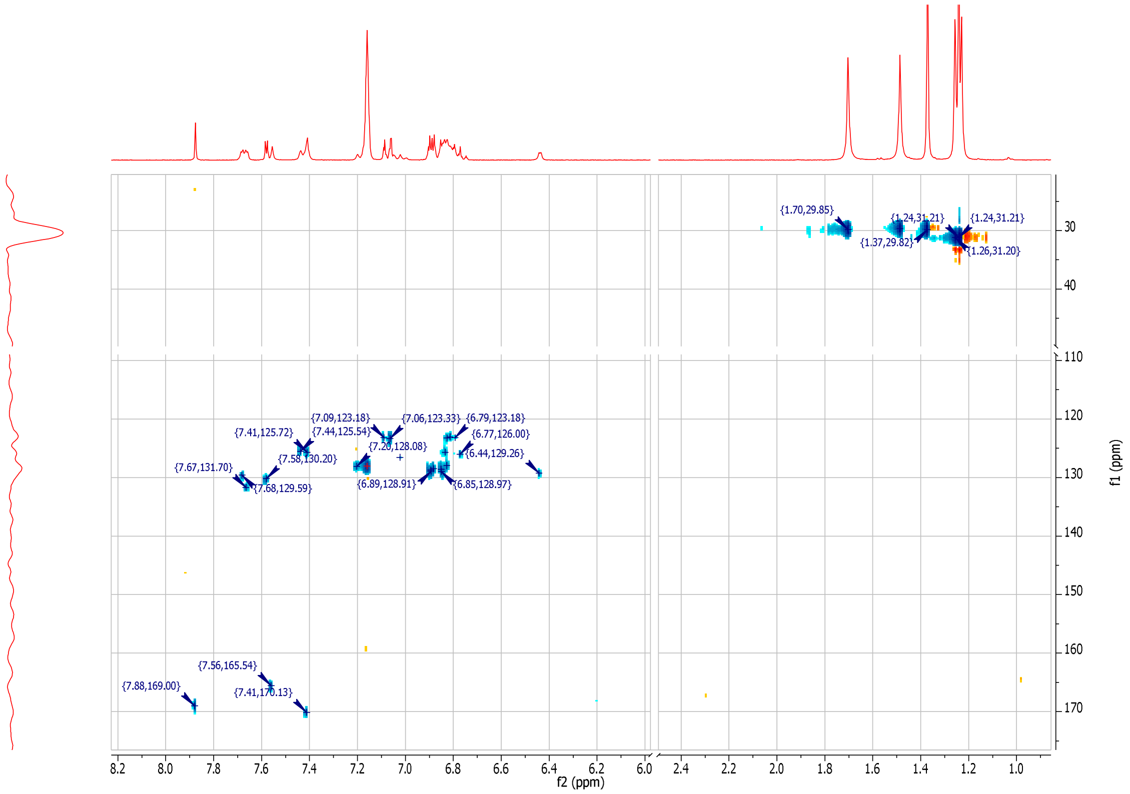

Figure S5. HSQC NMR spectrum of complex **2** $[MoO_2(L2)_2]$ in C_6D_6. The resonances were assigned to the two isomers with respect to their intensity.

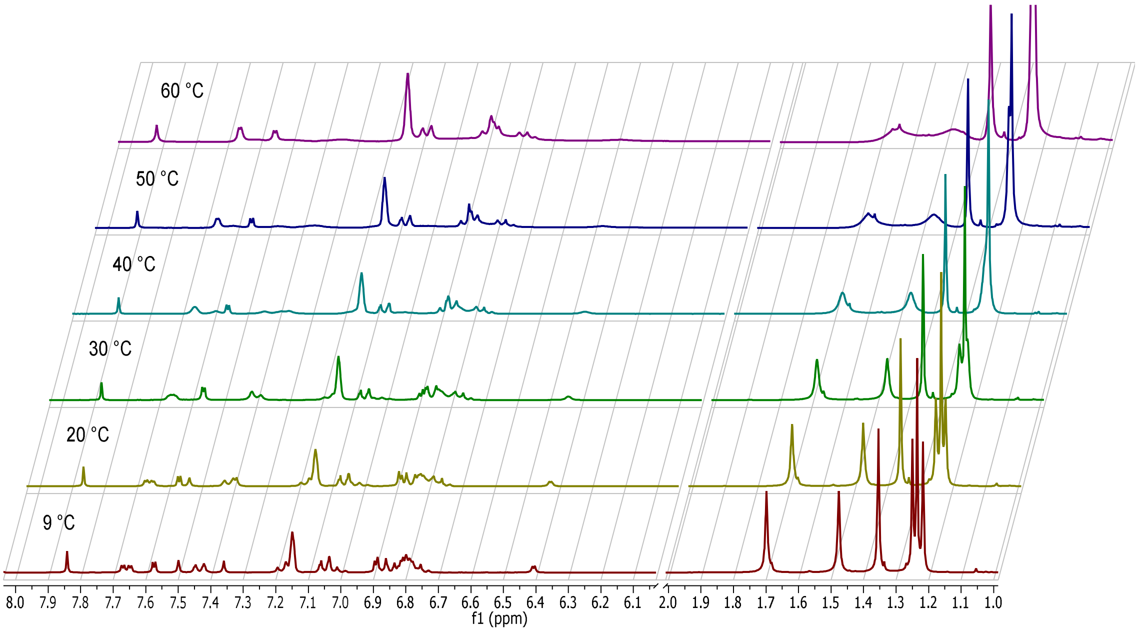

Figure S6. VT NMR spectrum of complex **2** $[MoO_2(L2)_2]$ in C_6D_6 from 9 °C to 60 °C in steps of 10 °C.

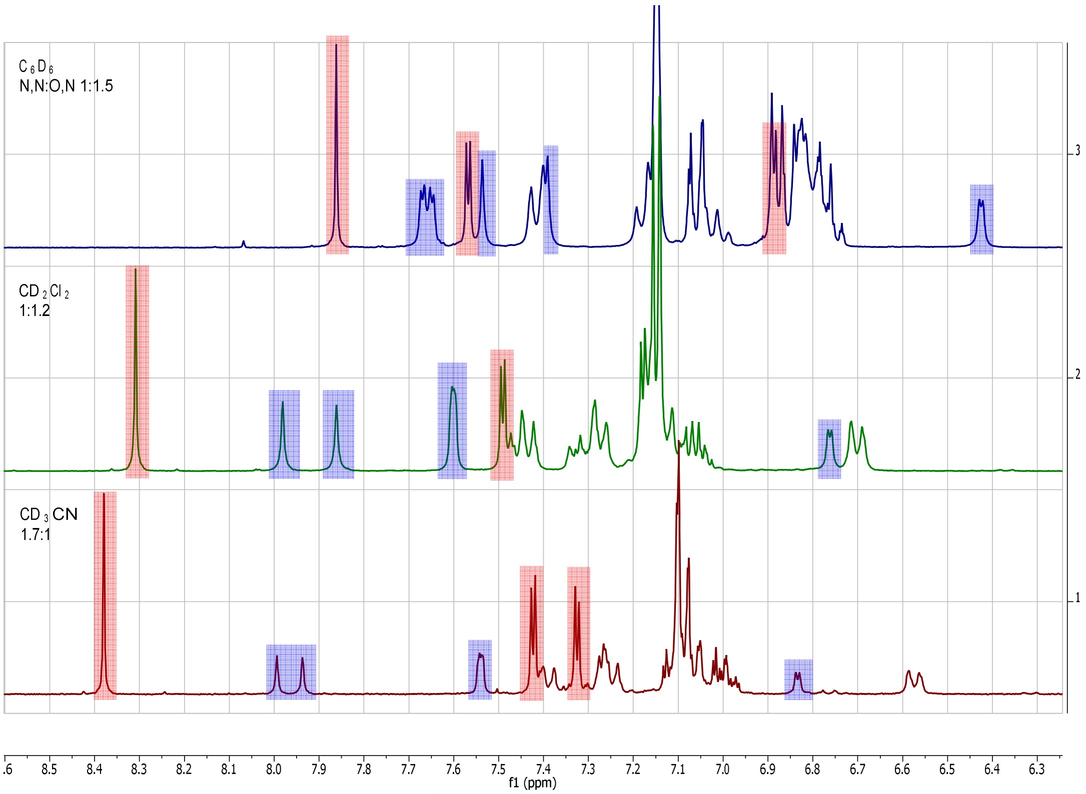

Figure S7. Aromatic region of ^{1}H NMR spectra of complex **2** [$MoO_2(L2)_2$] in C_6D_6 (top), CD_2Cl_2 (middle) and CD_3CN (bottom) with the corresponding isomeric ratios. Representative imine and phenolate proton resonances for the respective isomers are highlighted in red (N,N isomer) and blue (O,N isomer).

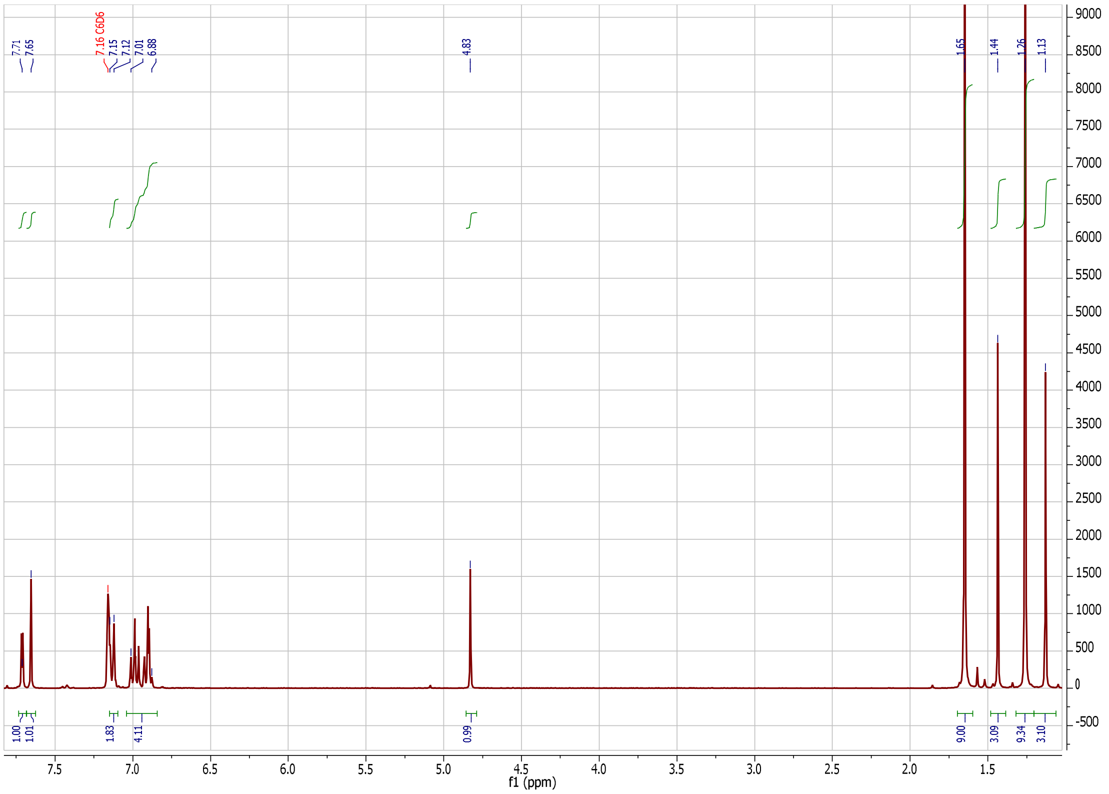

Figure S8. Proton NMR spectrum of complex **3** [$MoO_2(acac)(L2)$] in C_6D_6.

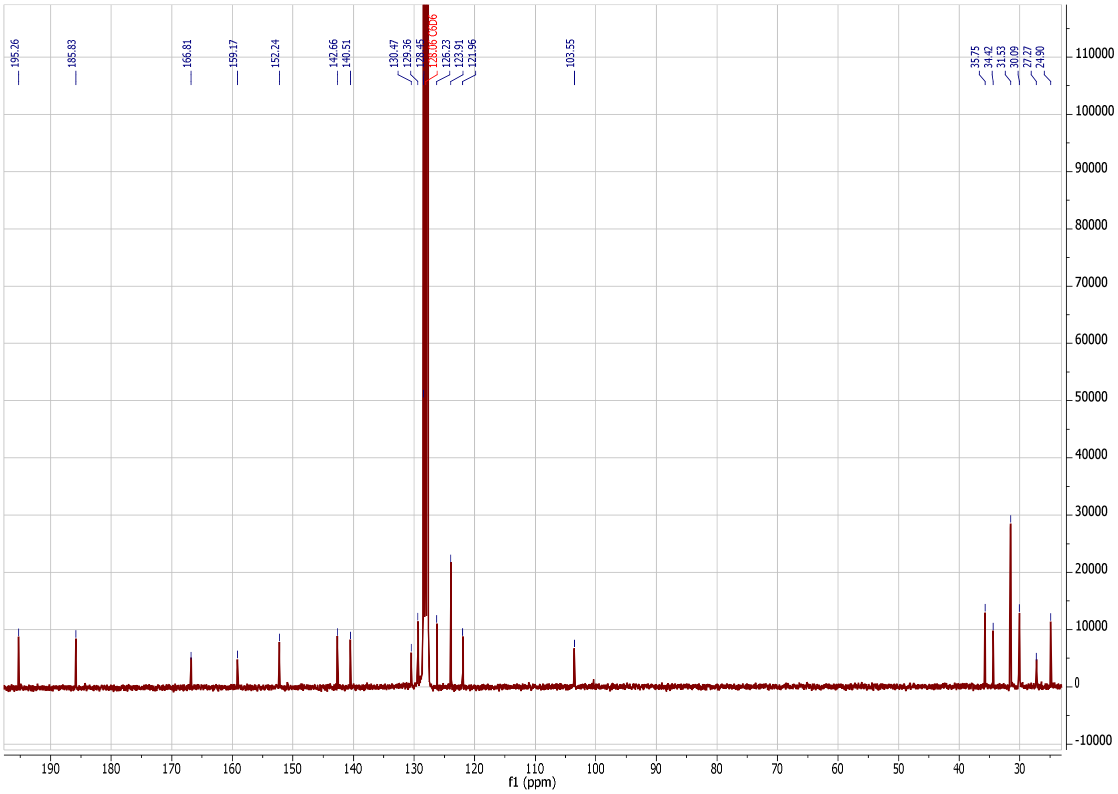

Figure S9. Carbon NMR spectrum of complex **3** [MoO_2(acac)(L2)] in C_6D_6.

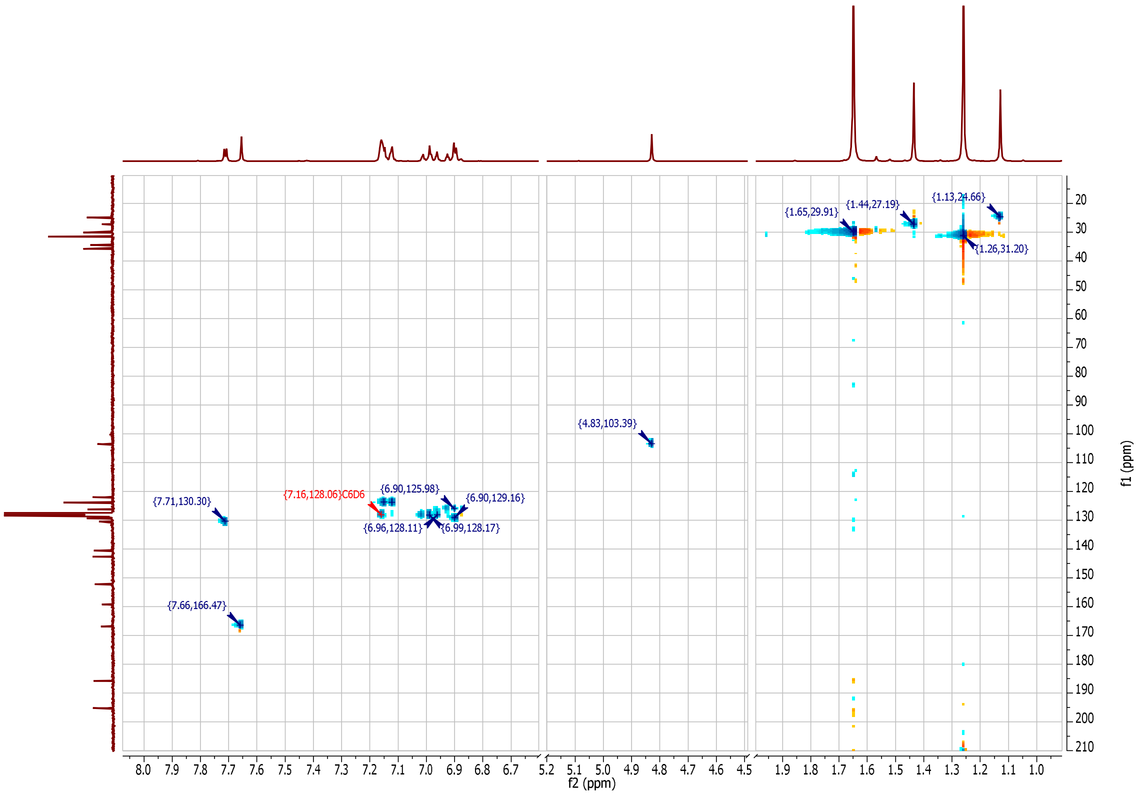

Figure S10. HSQC NMR spectrum of complex **3** [MoO_2(acac)(L2)] in C_6D_6.

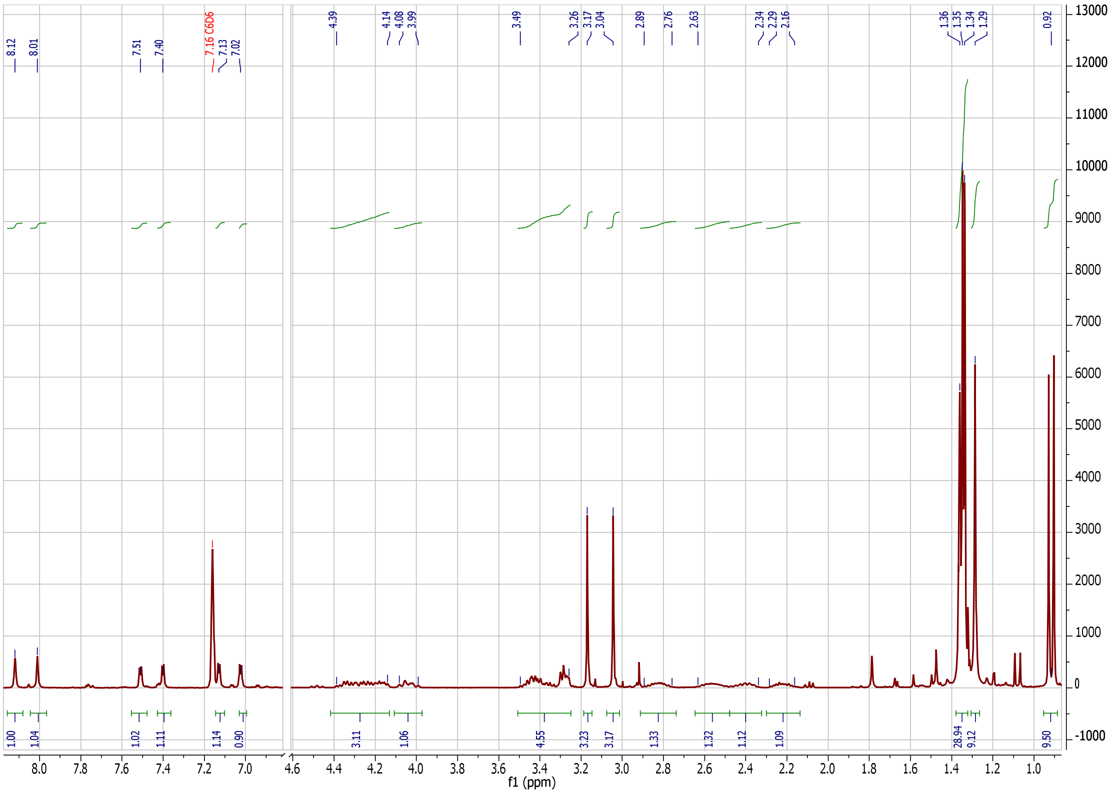

Figure S11. Proton NMR spectrum of the isomeric mixture of complex **4** $[MoO_2(PMe_3)(L1)_2]$ in C_6D_6.

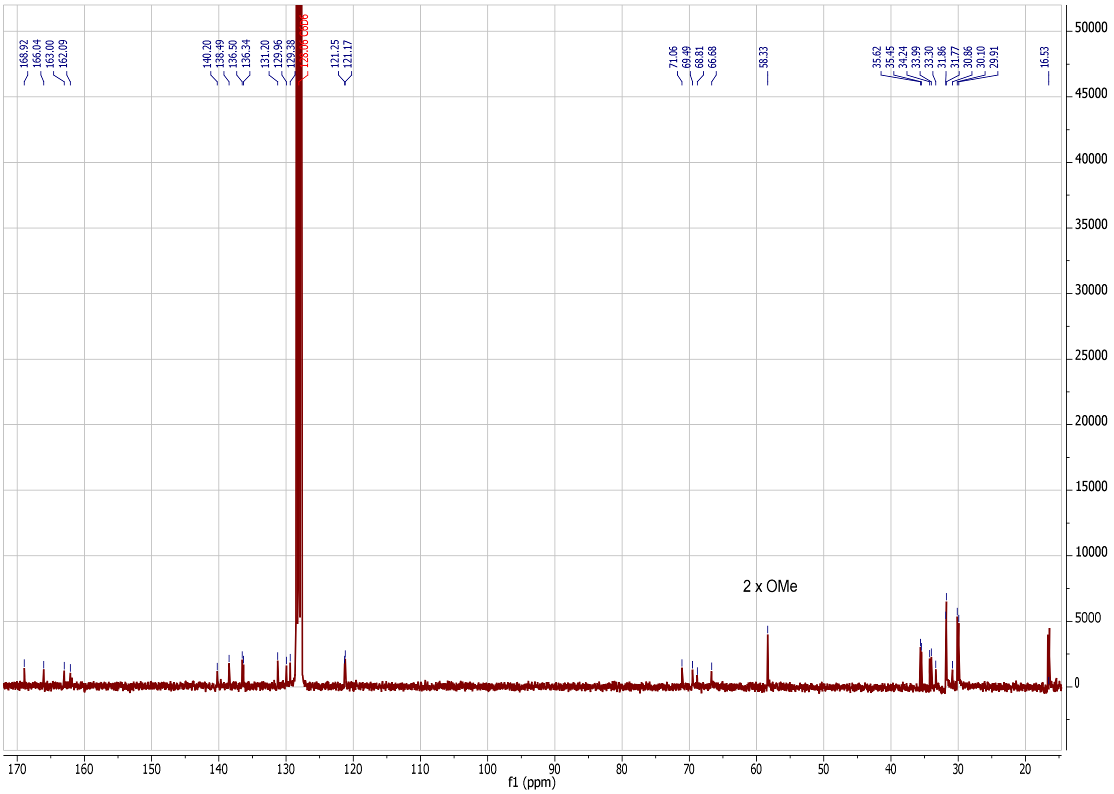

Figure S12. Carbon NMR spectrum of the isomeric mixture of complex **4** $[MoO_2(PMe_3)(L1)_2]$ in C_6D_6.

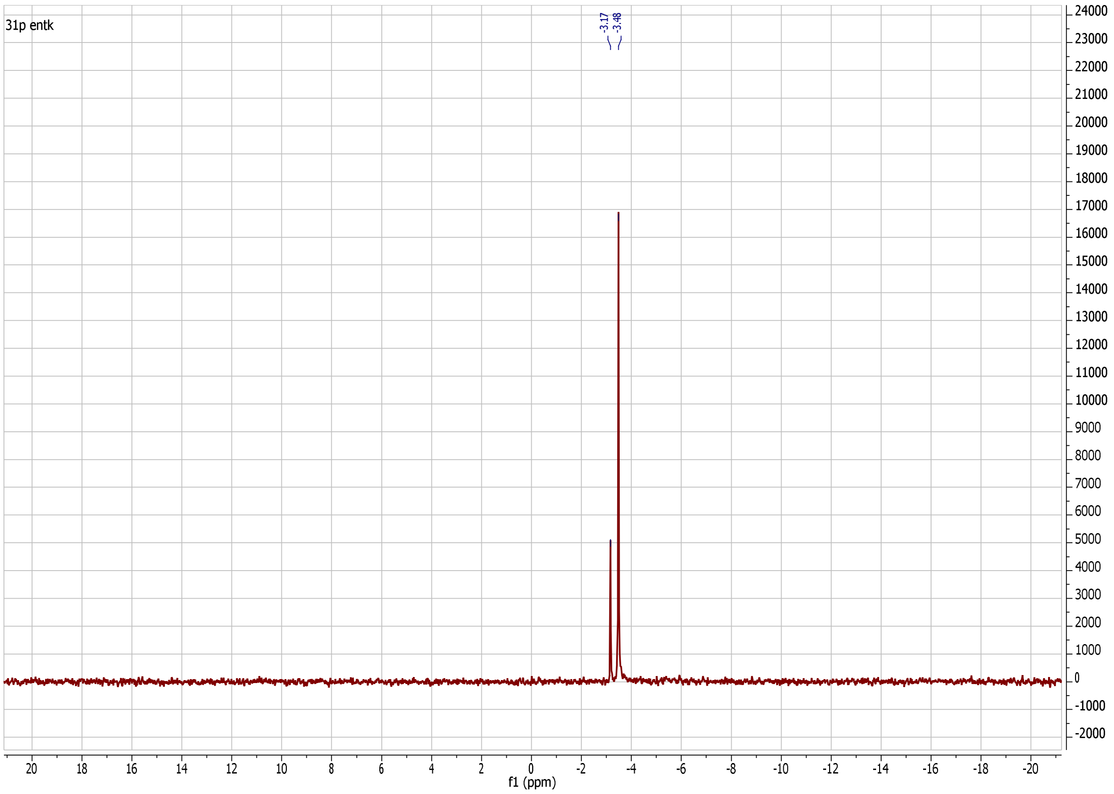

Figure S13. Phosphorus NMR spectrum of the isomeric mixture of complex **4** [$MoO_2(PMe_3)(L1)_2$] in C6D6.

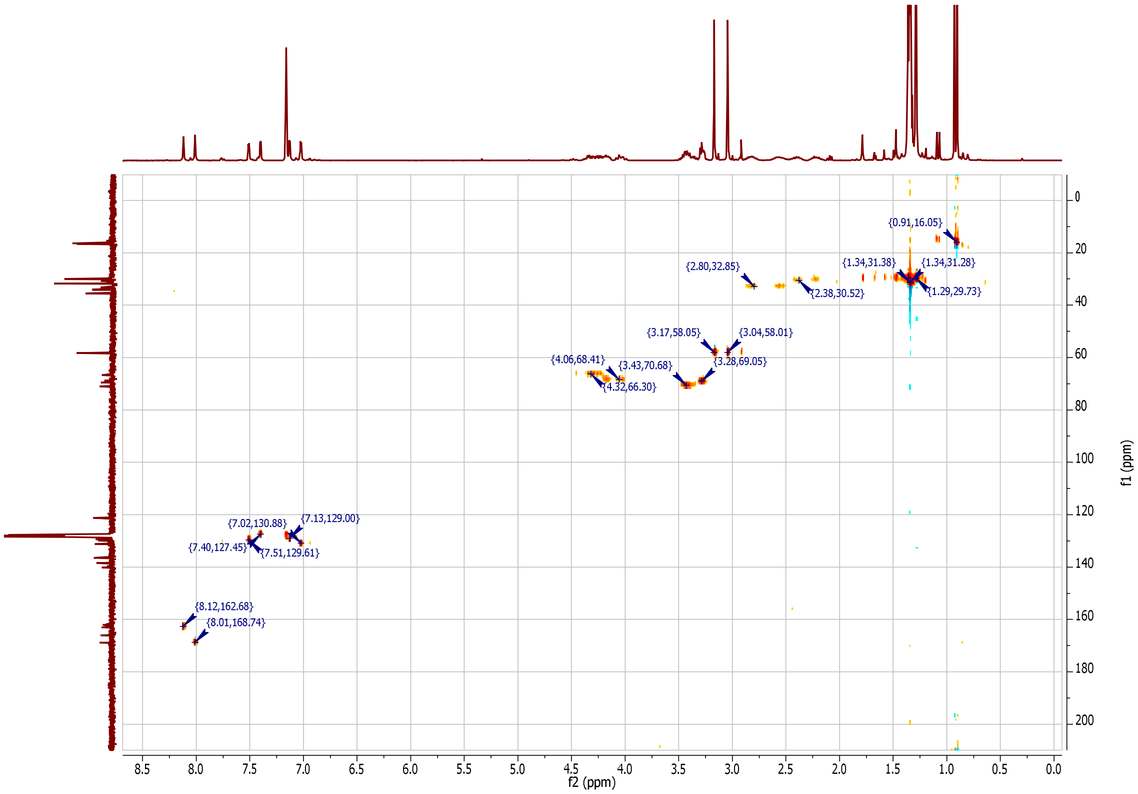

Figure S14. HSQC NMR spectrum of the isomeric mixture of complex **4** [$MoO_2(PMe_3)(L1)_2$] in C_6D_6.

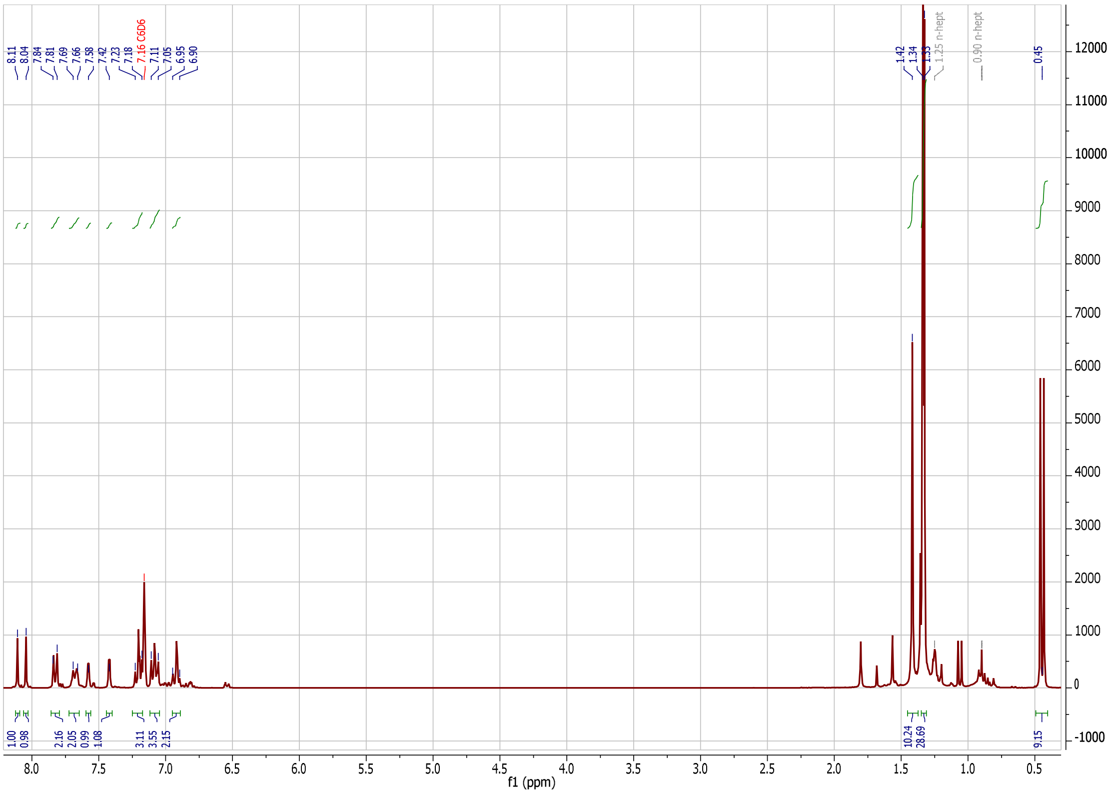

Figure S15. Proton NMR spectrum of the isomeric mixture of complex **5** [$MoO_2(PMe_3)(L2)_2$] in C_6D_6.

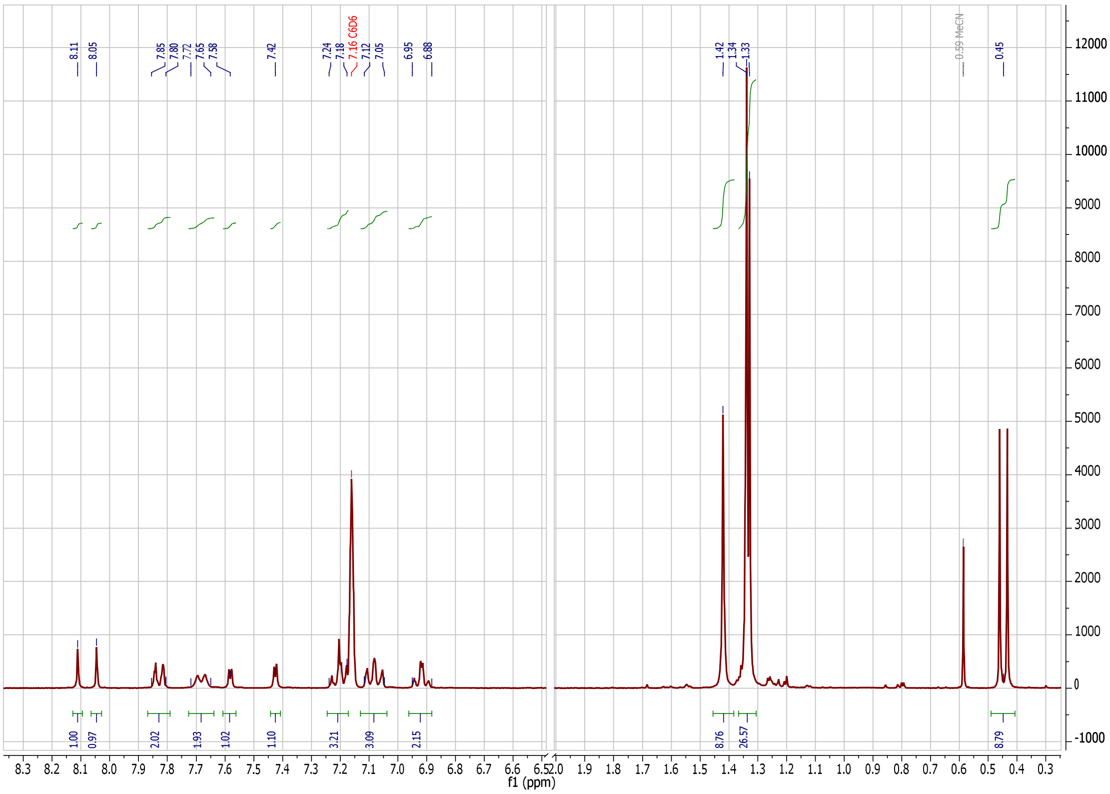

Figure S16. Proton NMR spectrum of the pure O,O isomer of of complex **5** [$MoO_2(PMe_3)(L2)_2$] in C_6D_6, obtained via recrystallization from MeCN.

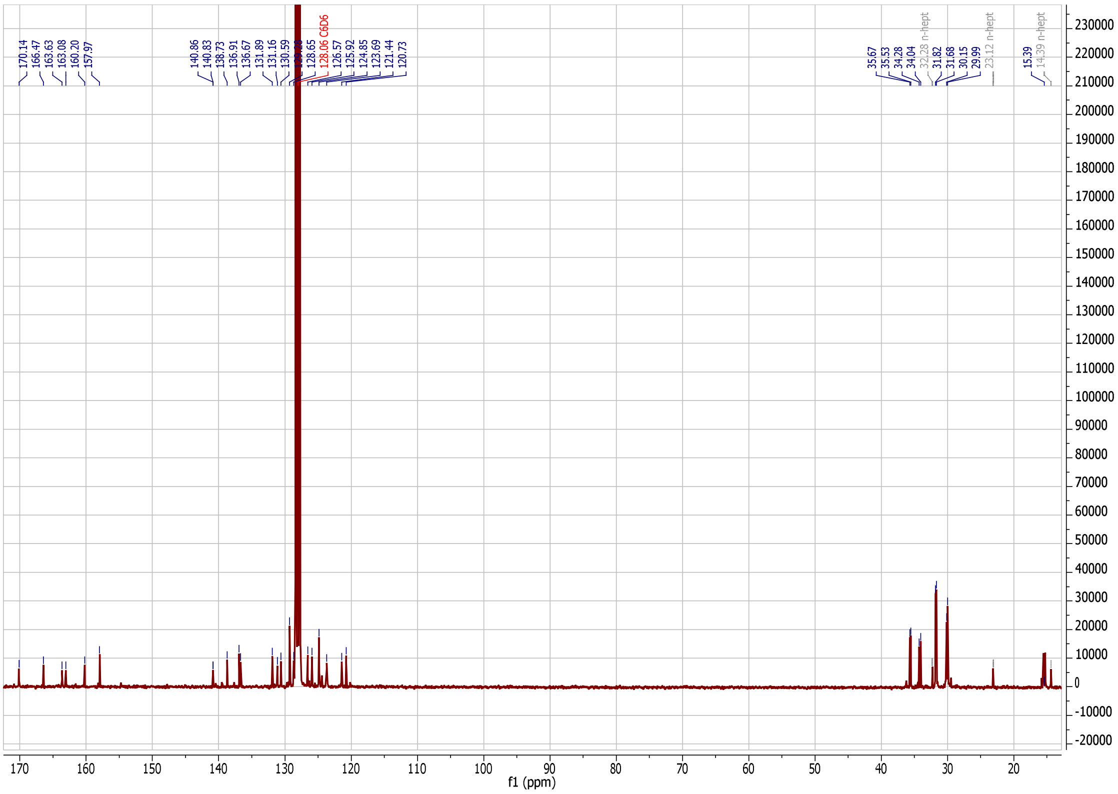

Figure S17. Carbon NMR spectrum of the isomeric mixture of complex **5** [$MoO_2(PMe_3)(L2)_2$] in C_6D_6.

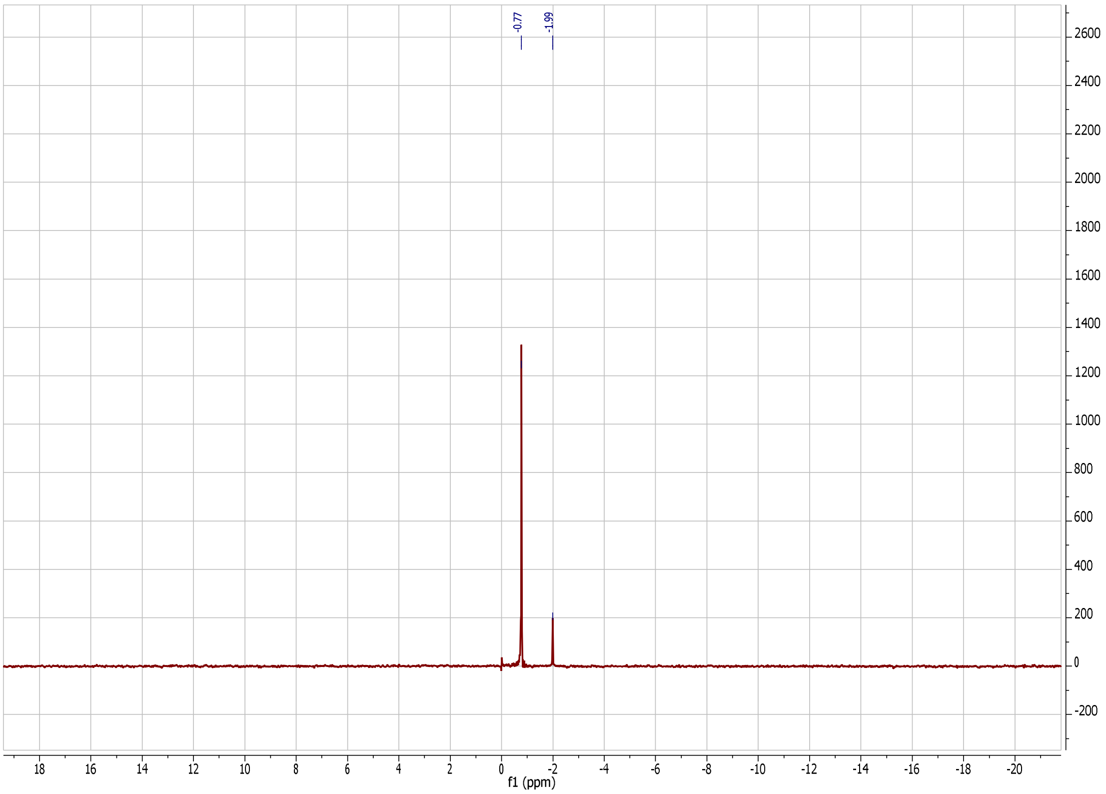

Figure S18. Phosphorus NMR spectrum of the isomeric mixture of complex **5** [$MoO_2(PMe_3)(L2)_2$] in C_6D_6.

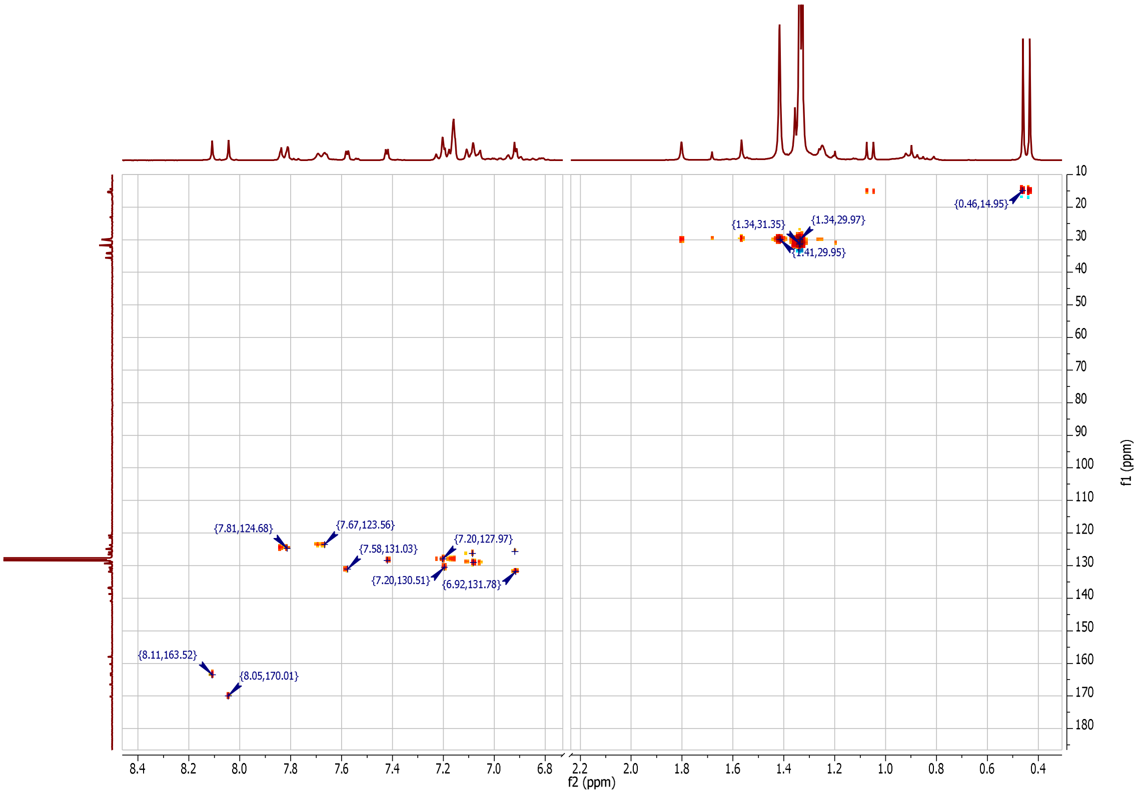

Figure S19. HSQC NMR spectrum of the isomeric mixture of complex **5** [$MoO_2(PMe_3)(L2)_2$] in C_6D_6.

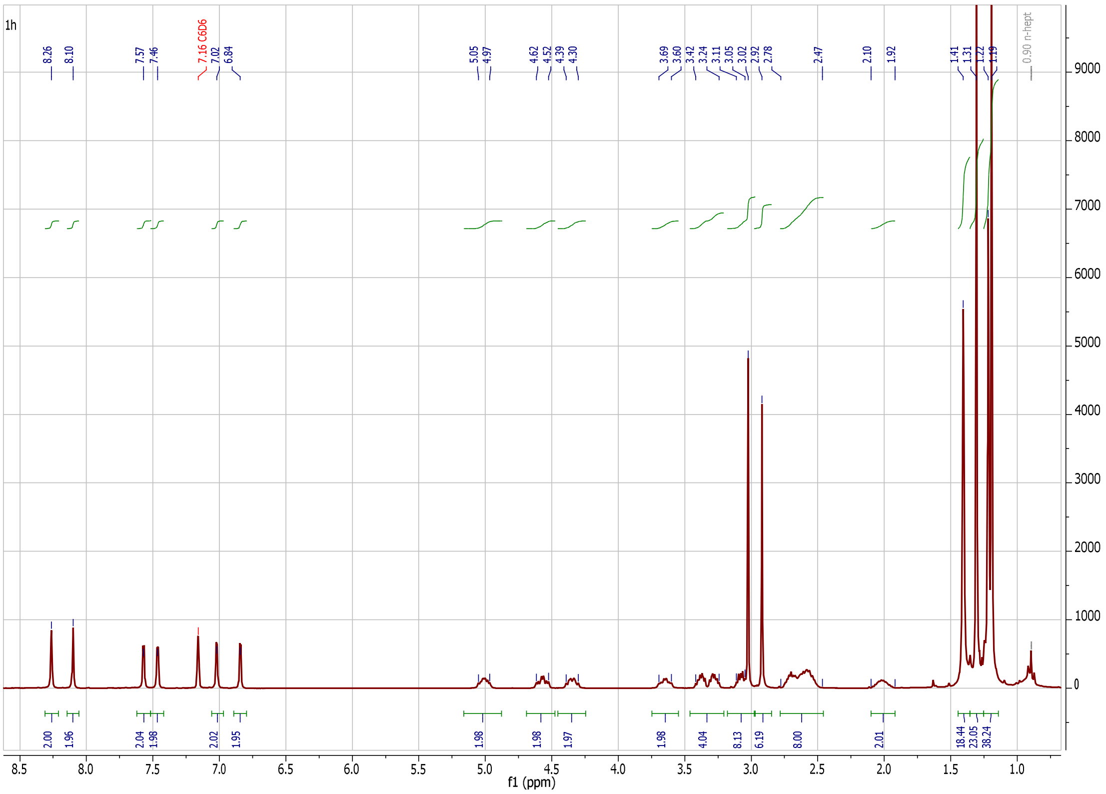

Figure S20. Proton NMR spectrum of complex **6** {[$MoO(L1)_2]_2(\mu\text{-}O)$} in C_6D_6.

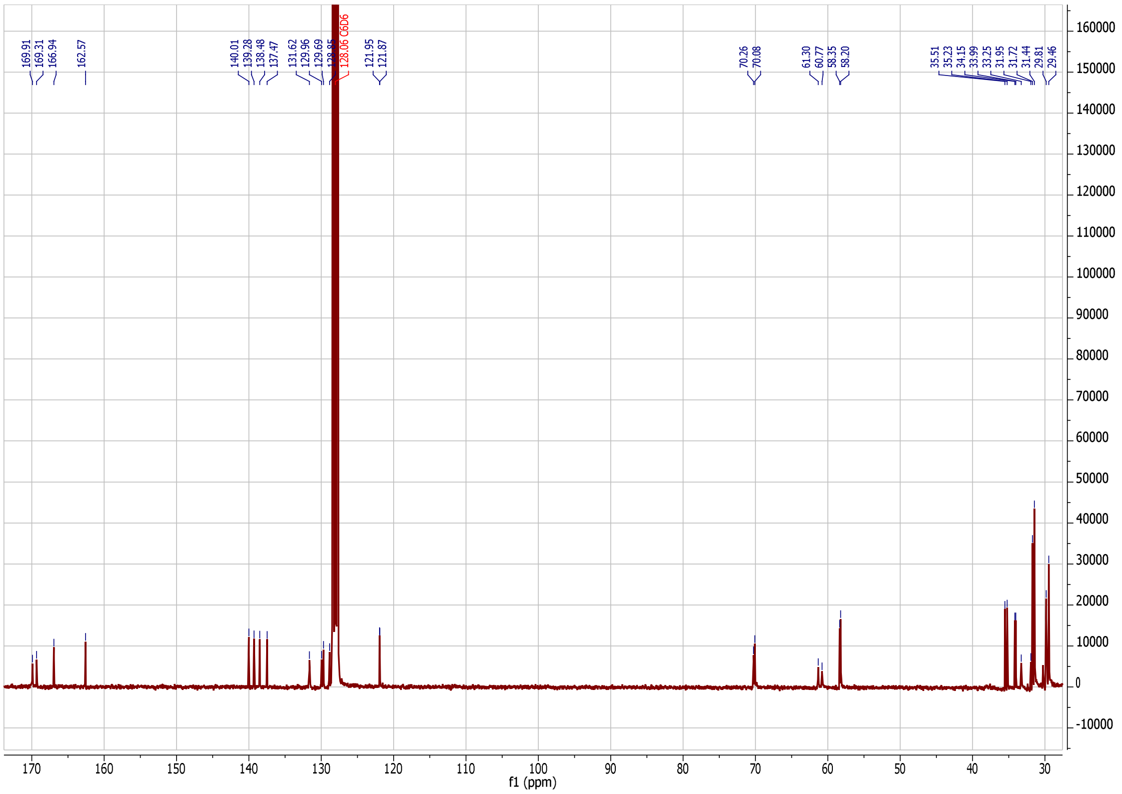

Figure S21. Carbon NMR spectrum of complex **6** {[MoO(L1)$_2$]$_2$(μ-O)} in C_6D_6.

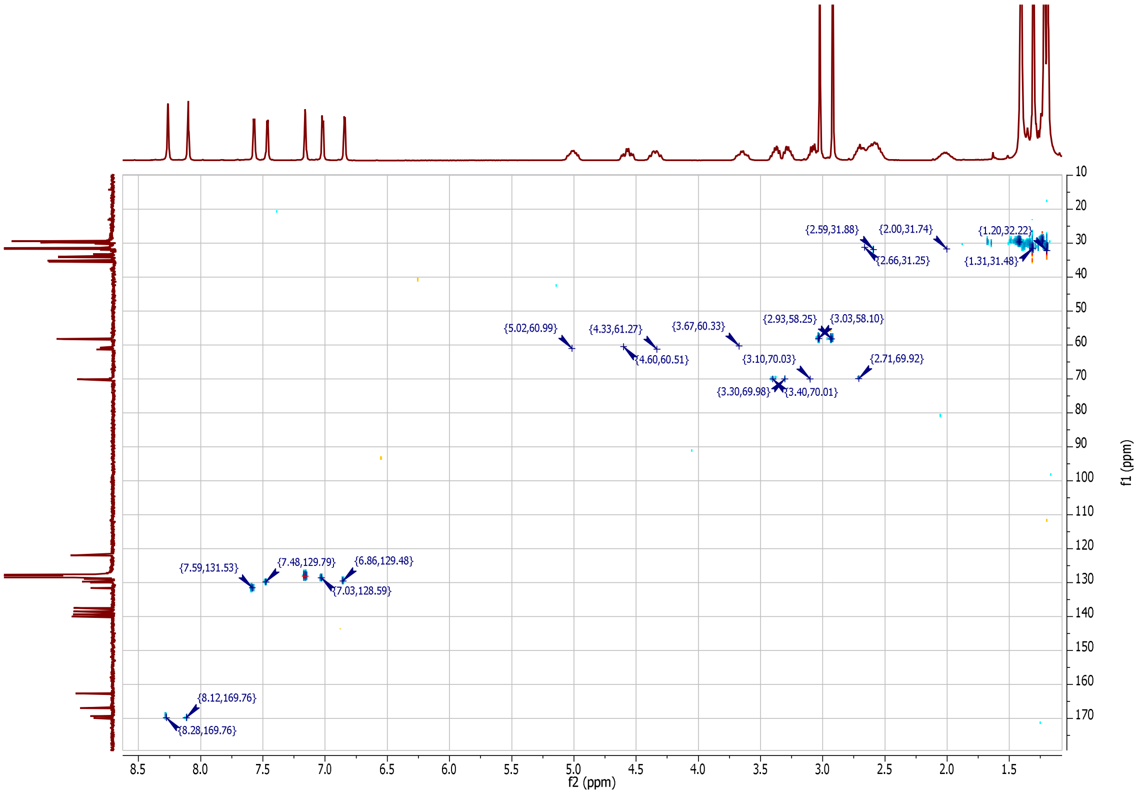

Figure S22. HSQC NMR spectrum of complex **6** {[MoO(L1)$_2$]$_2$(μ-O)} in C_6D_6.

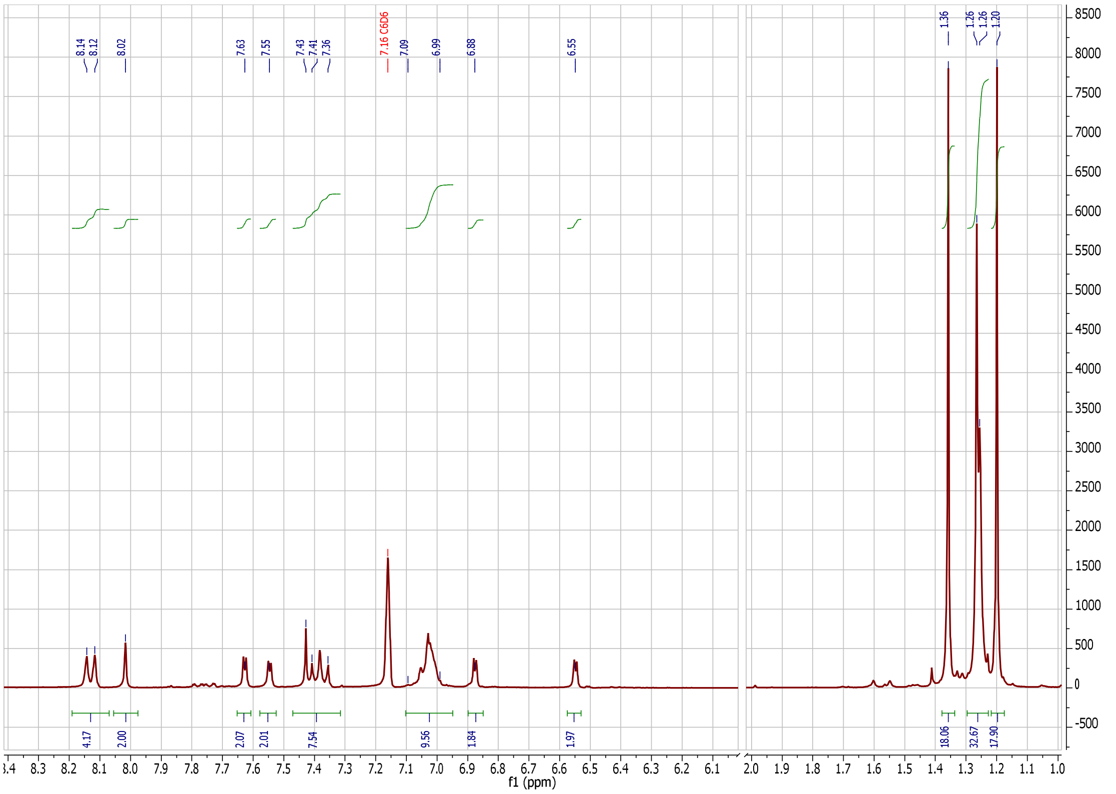

Figure S23. Proton NMR spectrum of complex **7** {[MoO(L2)$_2$]$_2$(μ-O)} in C_6D_6.

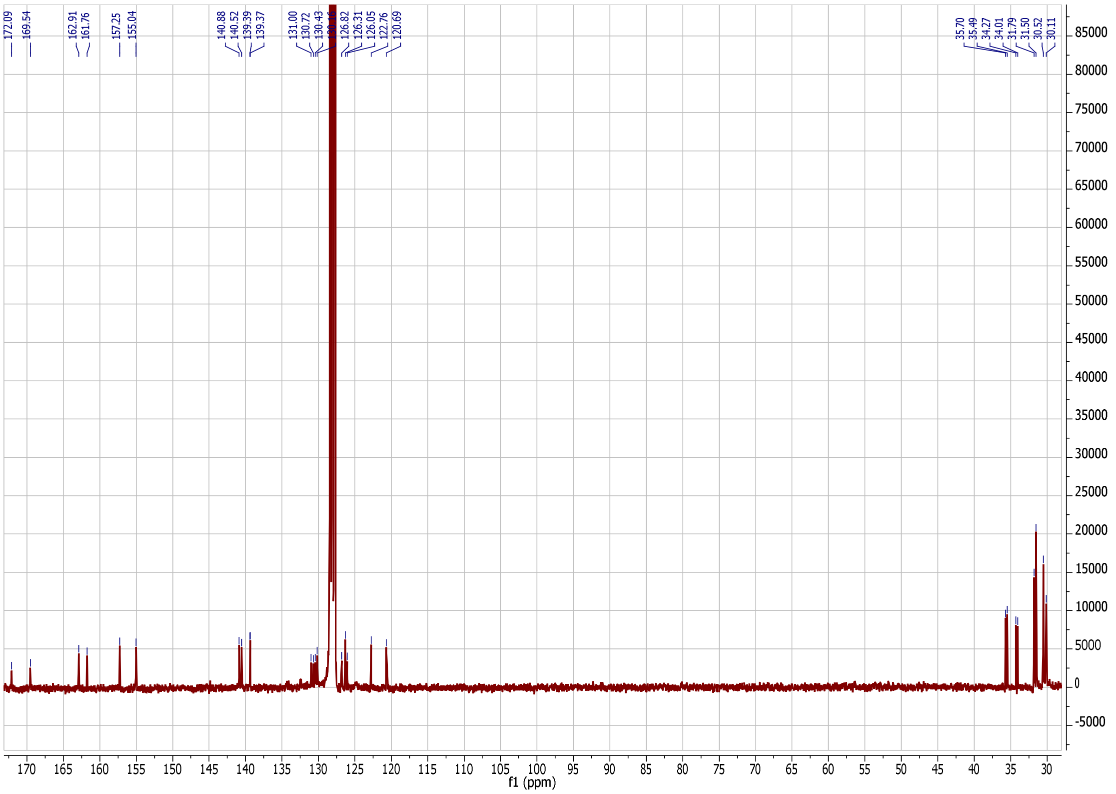

Figure S24. Carbon NMR spectrum of complex **7** {[MoO(L2)$_2$]$_2$(μ-O)} in C_6D_6.

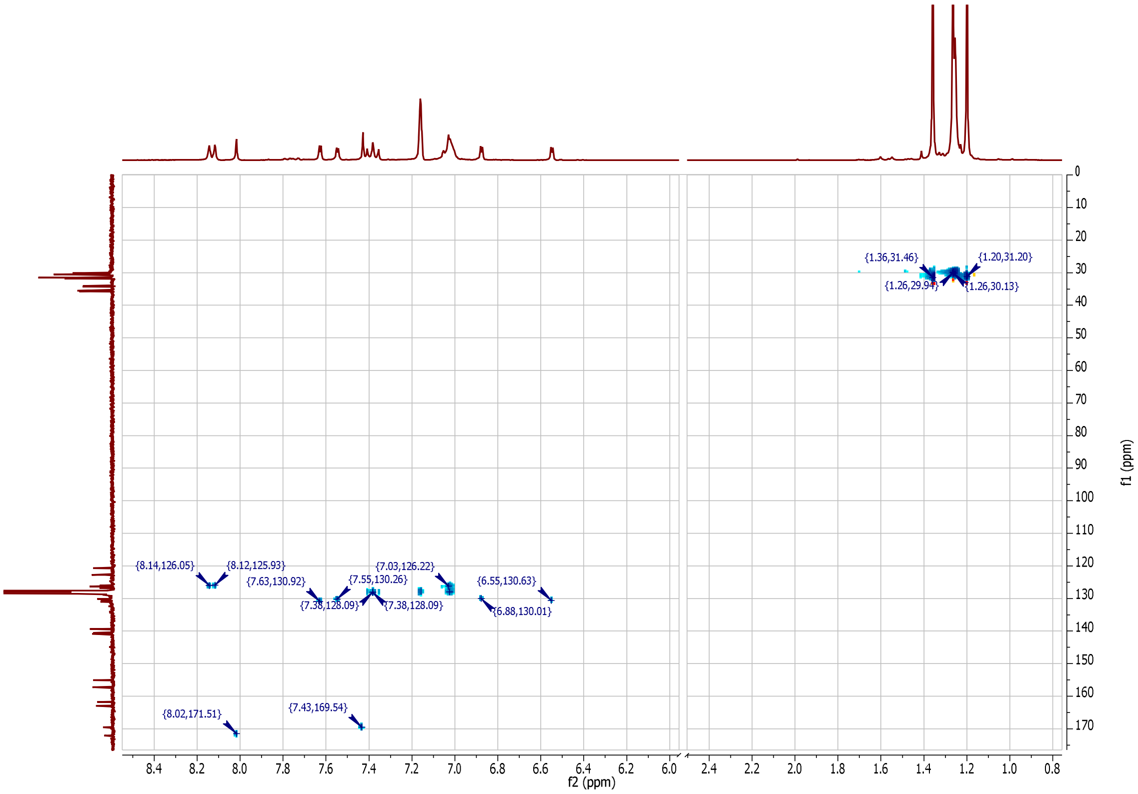

Figure S25. HSQC NMR spectrum of complex **7** {[MoO(L2)$_2$]$_2$(μ-O)} in C$_6$D$_6$.

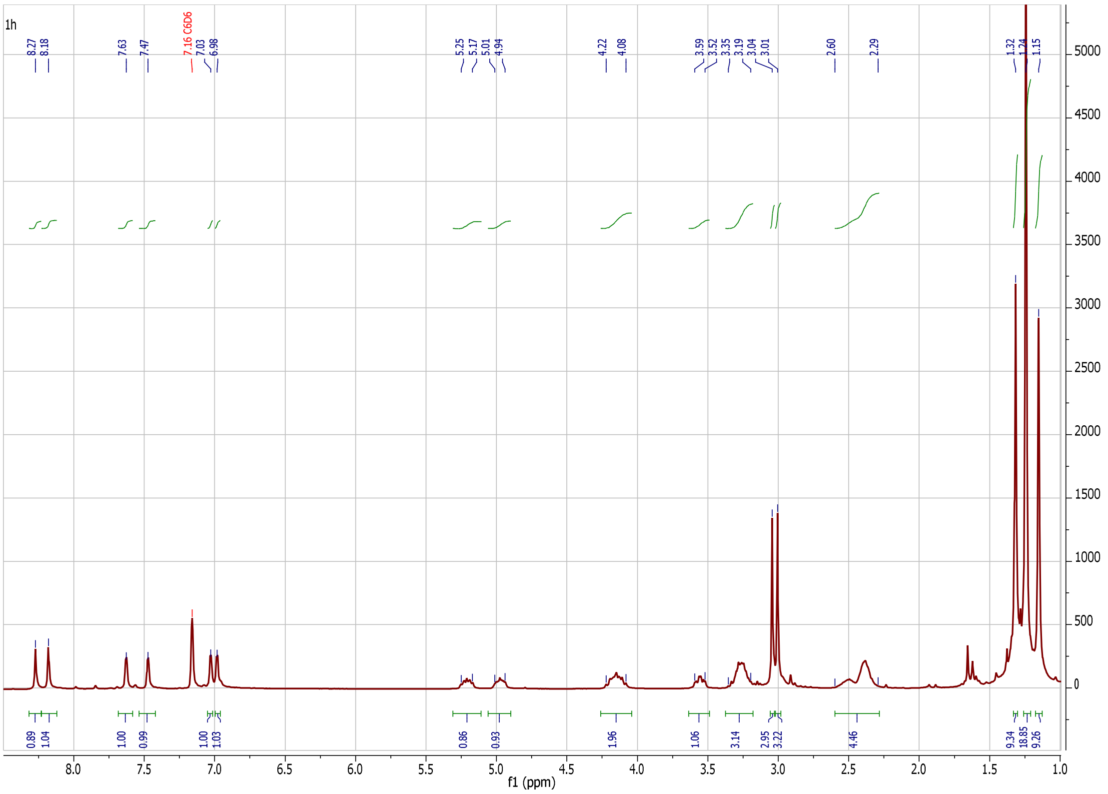

Figure S26. Proton NMR spectrum of complex **8** [MoO(O$_2$)(L1)$_2$] in C6D6.

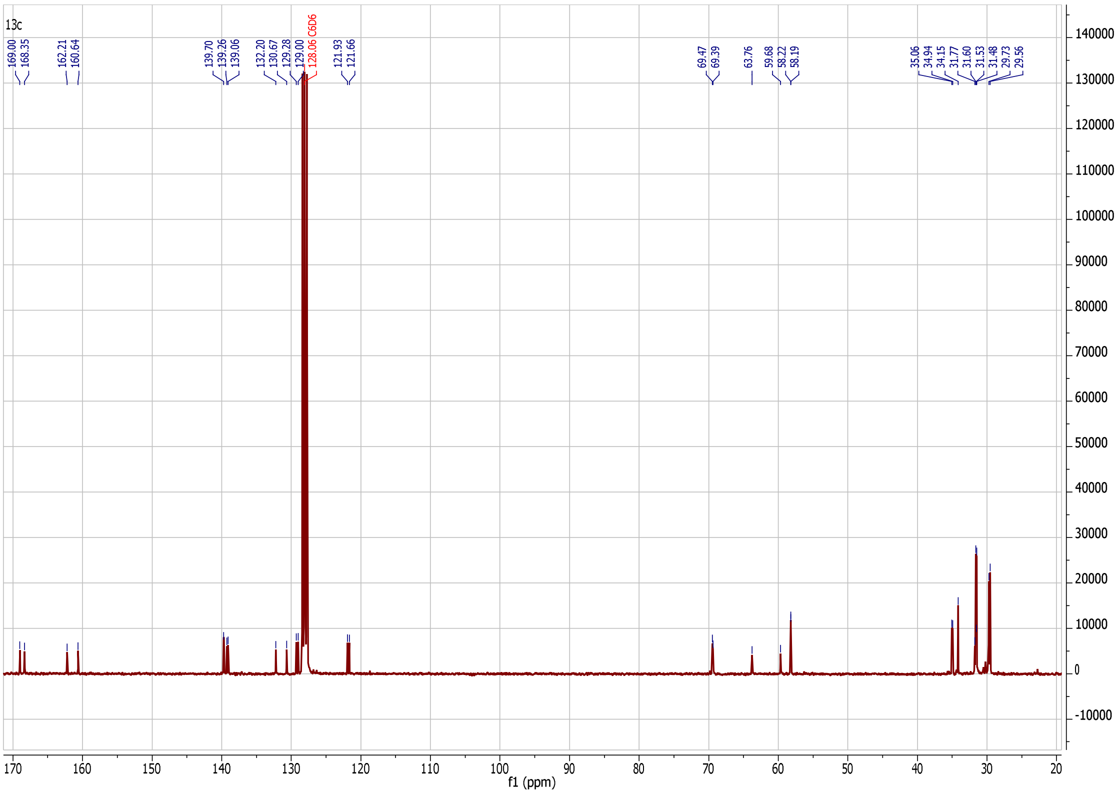

Figure S27. Carbon NMR spectrum of complex **8** [MoO(O_2)(L1)$_2$] in C_6D_6.

Figure S28. HSQC NMR spectrum of complex **8** [MoO(O_2)(L1)$_2$] in C_6D_6.

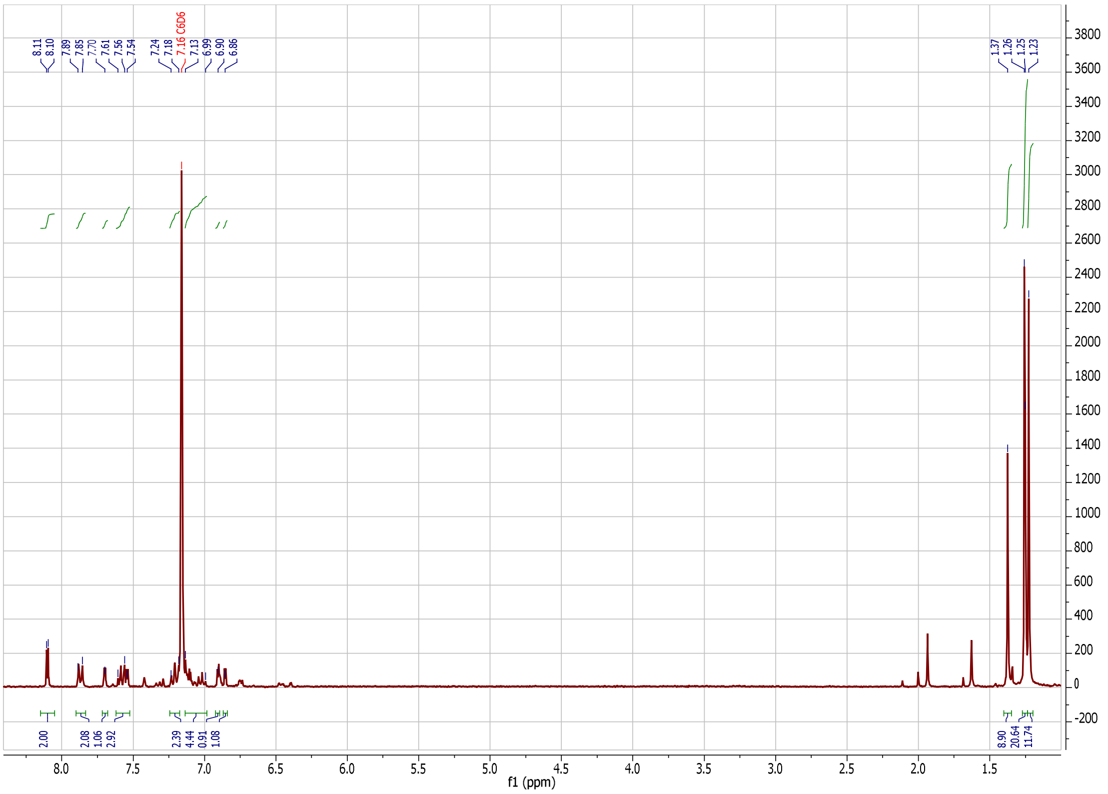

Figure S29. Proton NMR spectrum of the isomeric mixture of complex **9** [$MoO(O_2)(L2)_2$] in C_6D_6 with the O,O isomer assigned.

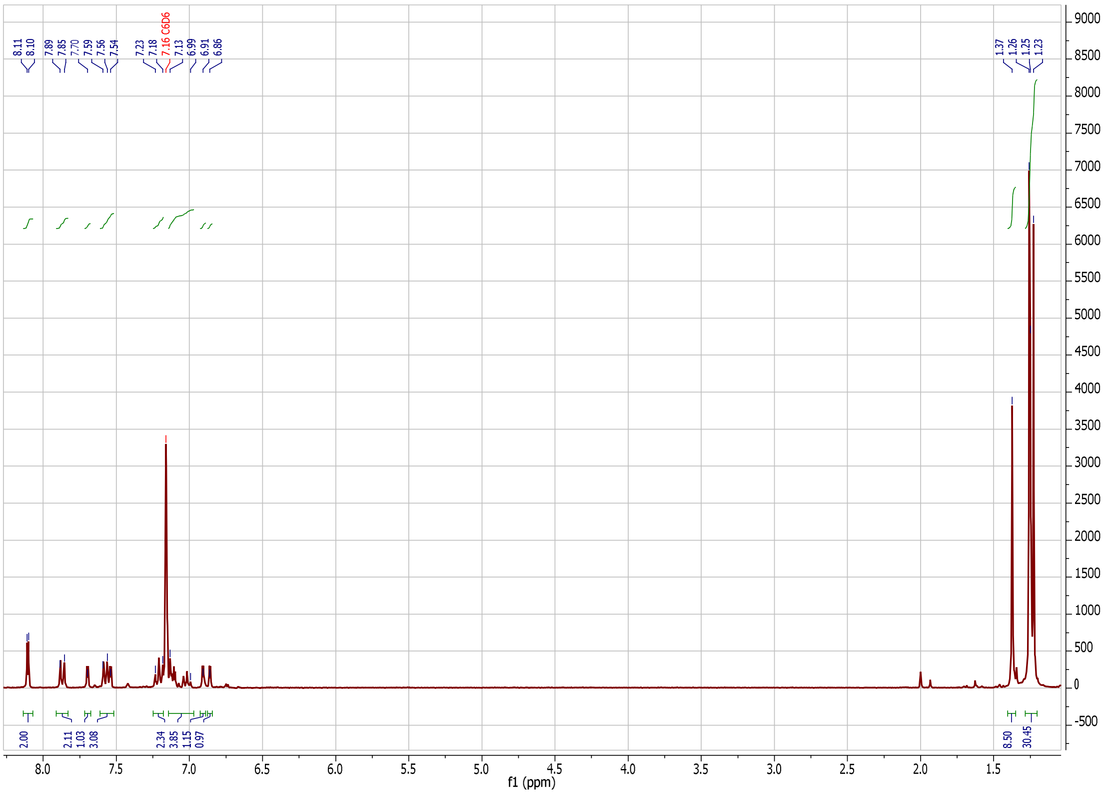

Figure S30. Proton NMR spectrum of the O,O isomer of complex **9** [$MoO(O_2)(L2)_2$] in C_6D_6 obtained via recrystallization from MeCN and immediate measurement.

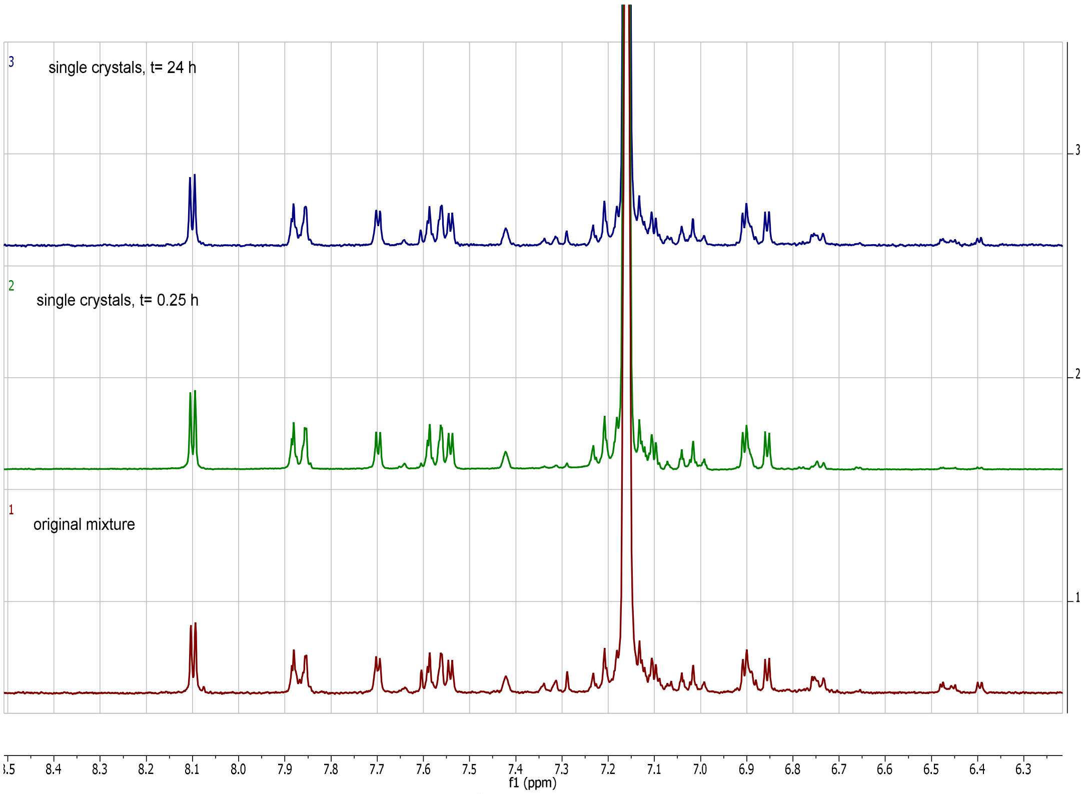

Figure S31. Aromatic region of the ^{1}H NMR spectra of the initial isomeric mixture and dissolved single crystals of **9** [MoO(O_2)(L2)$_2$] after t=0.25 h and t=24 h in C_6D_6 showing the isomeric equilibration.

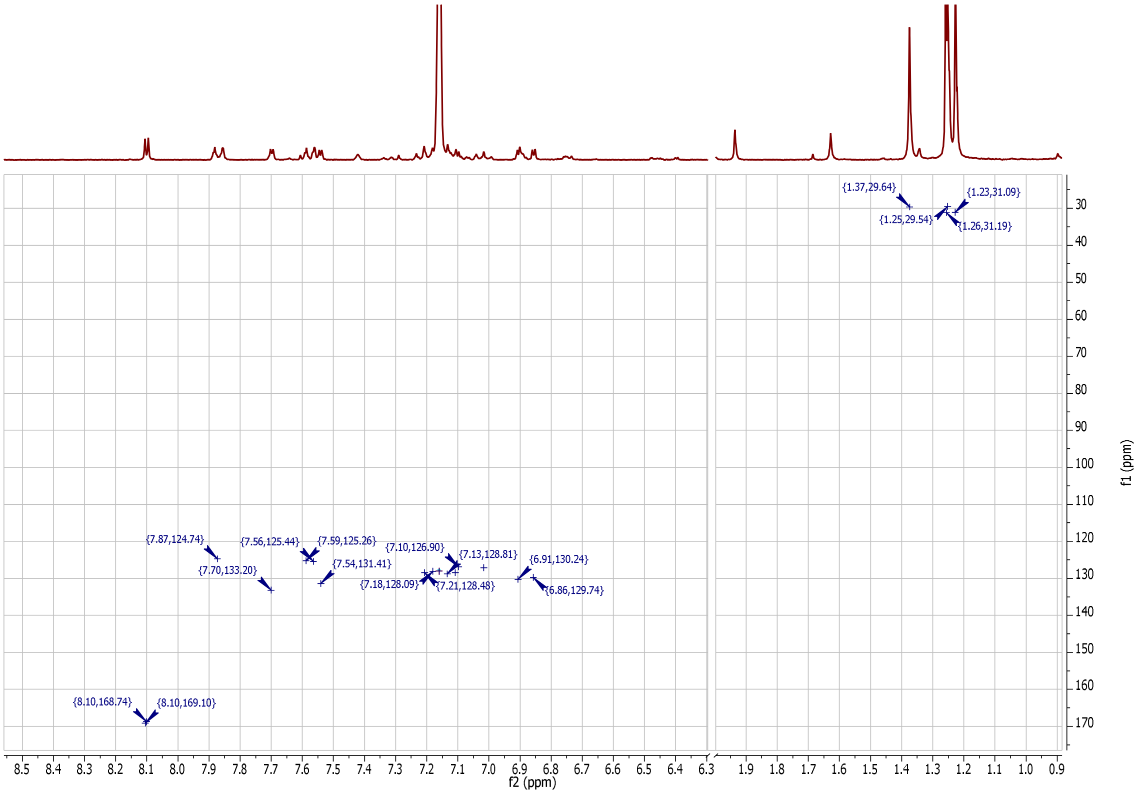

Figure S32. HSQC NMR spectrum of the isomeric mixture of complex **9** [MoO(O_2)(L2)$_2$] in C_6D_6 with the major isomer assigned.

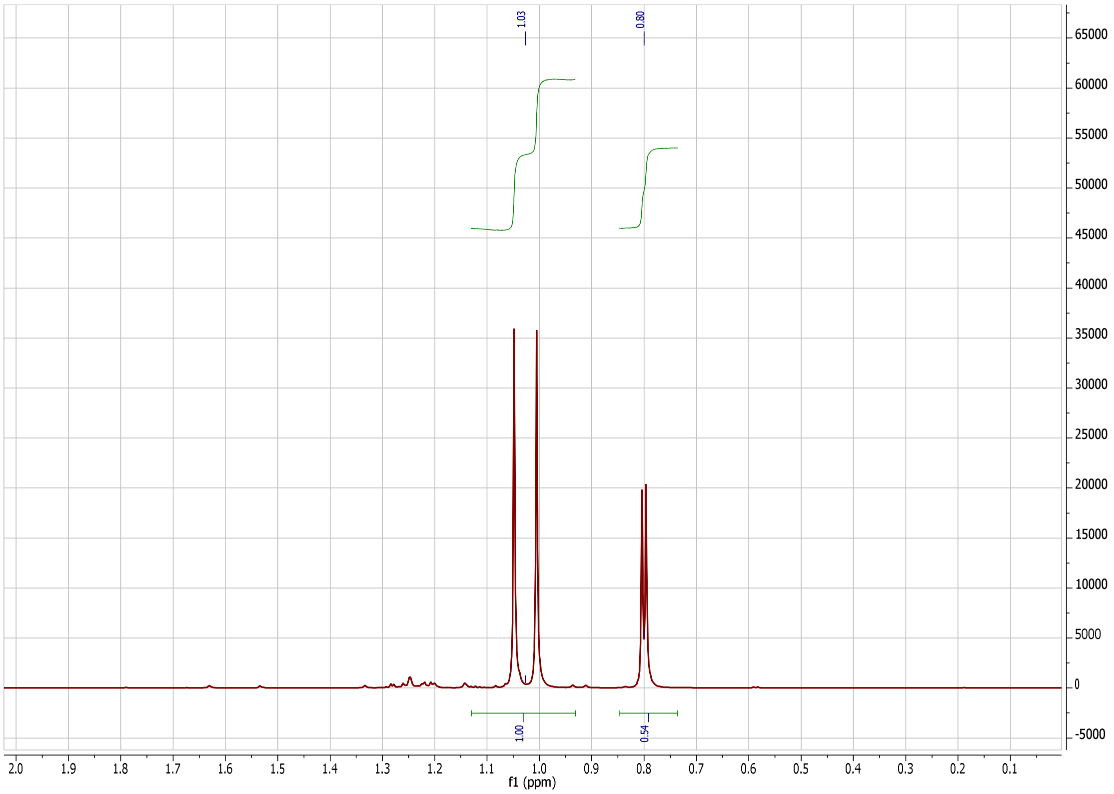

Figure S33. Proton NMR resonances of the catalytic aerobic oxidation of PMe_3 using 1 mol% of **1** under O_2 pressure (1.5 atm) in C_6D_6 at ambient conditions after t=24h; Depicted integrals correspond to the ratio of $OPMe_3$:PMe_3.

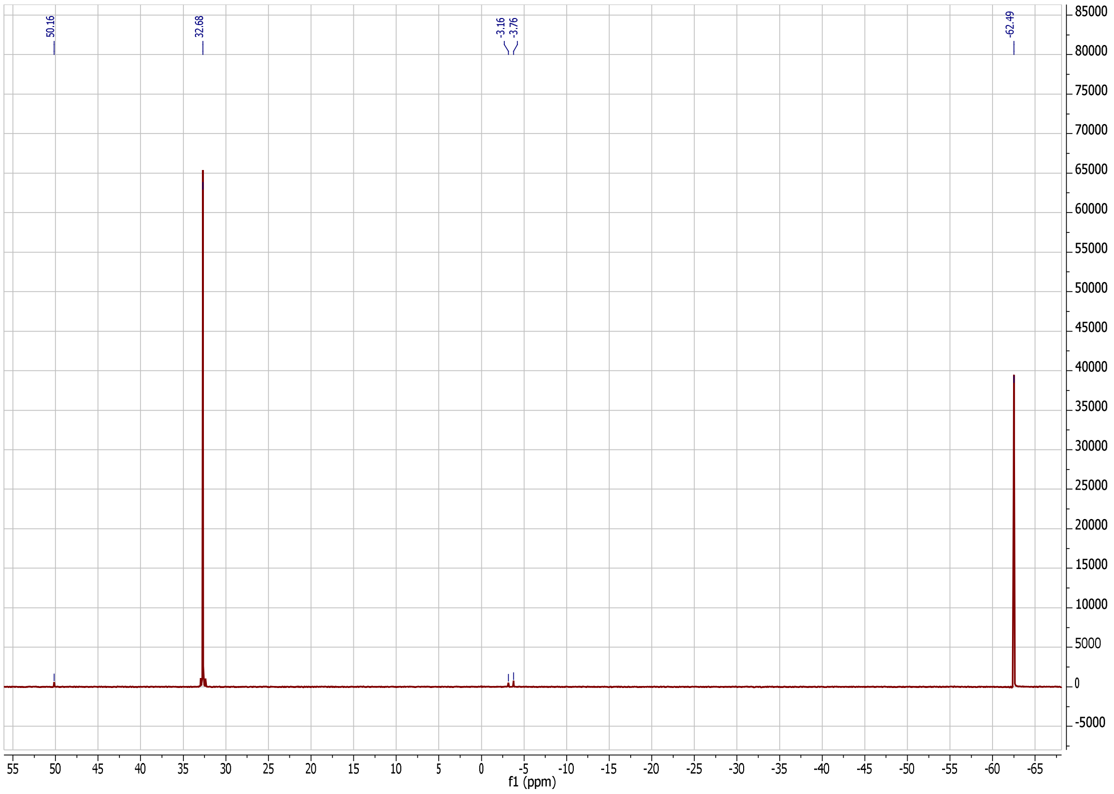

Figure S34. Phosphorus NMR resonances of the catalytic aerobic oxidation of PMe_3 using 1 mol% of **1** under O_2 pressure (1.5 atm) in C_6D_6 at ambient conditions after t=24h;

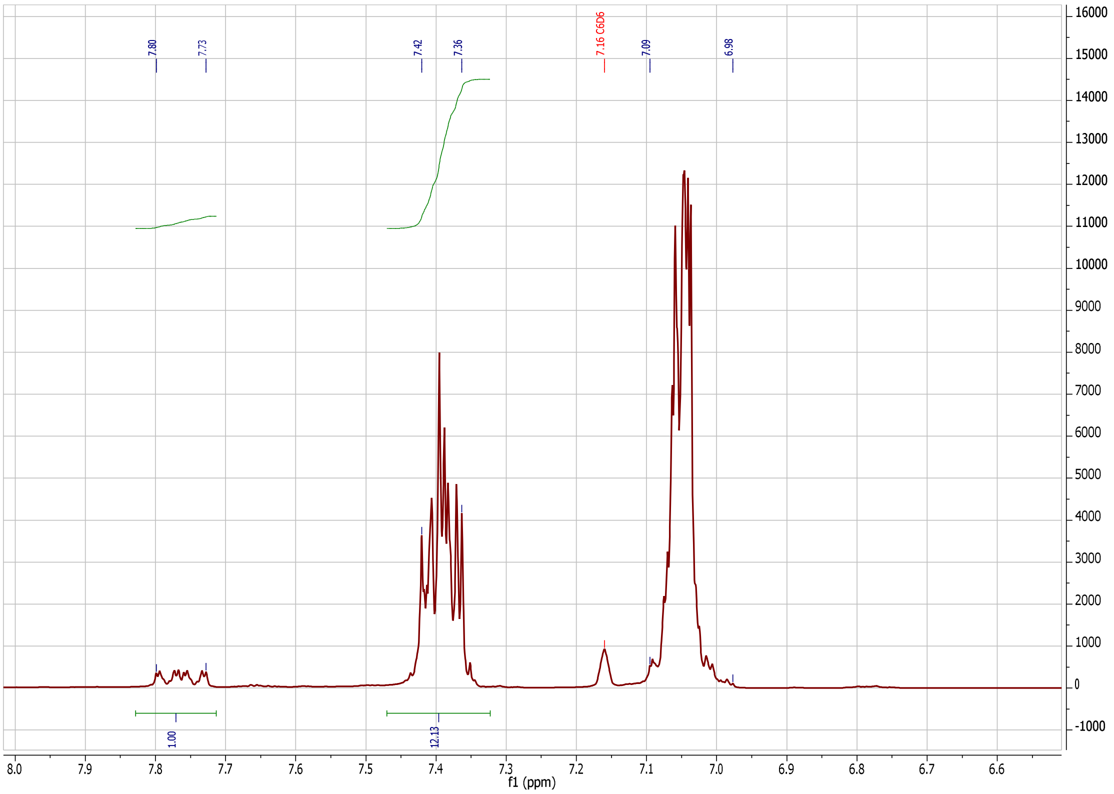

Figure S35. Proton NMR resonances of the catalytic aerobic oxidation of PPh_3 using 1 mol% of **1** under O_2 pressure (1.5 atm) in C_6D_6 at ambient conditions after t=24h; Depicted integrals correspond to the ratio of $OPPh_3$:PPh_3.

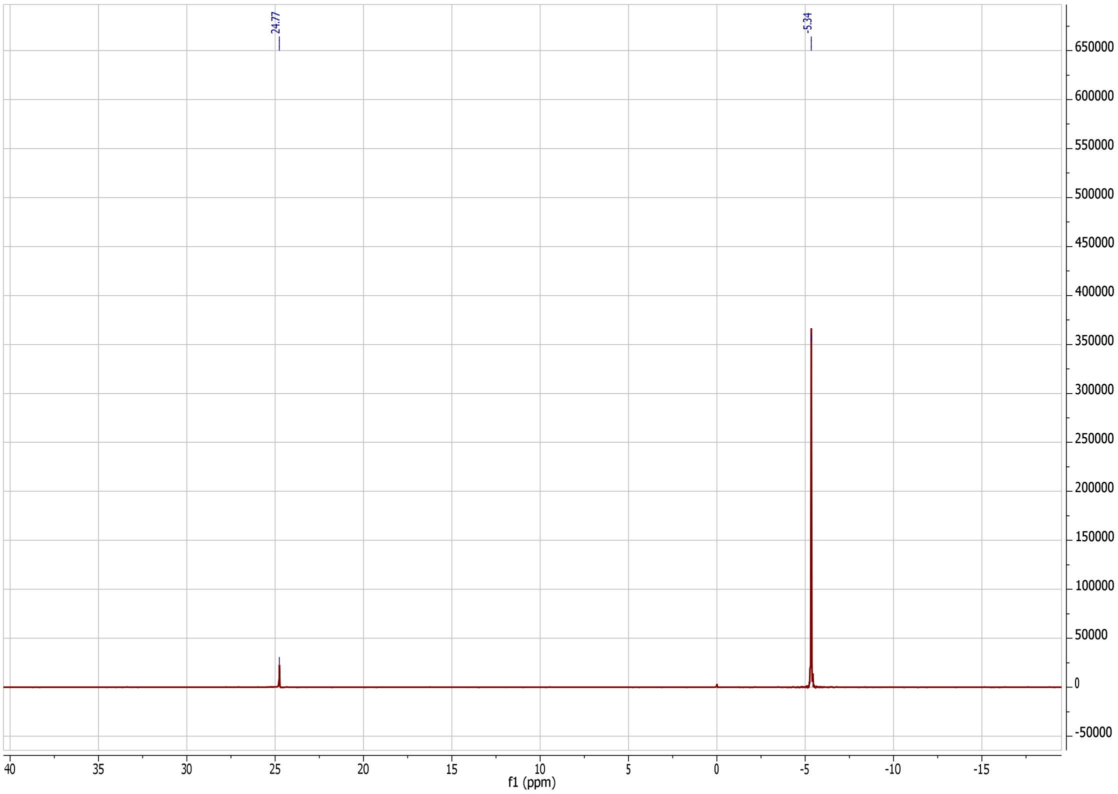

Figure S36. Phosphorus NMR resonances of the catalytic aerobic oxidation of PPh_3 using 1 mol% of **1** under O_2 pressure (1.5 atm) in C_6D_6 at ambient conditions after t=24h;

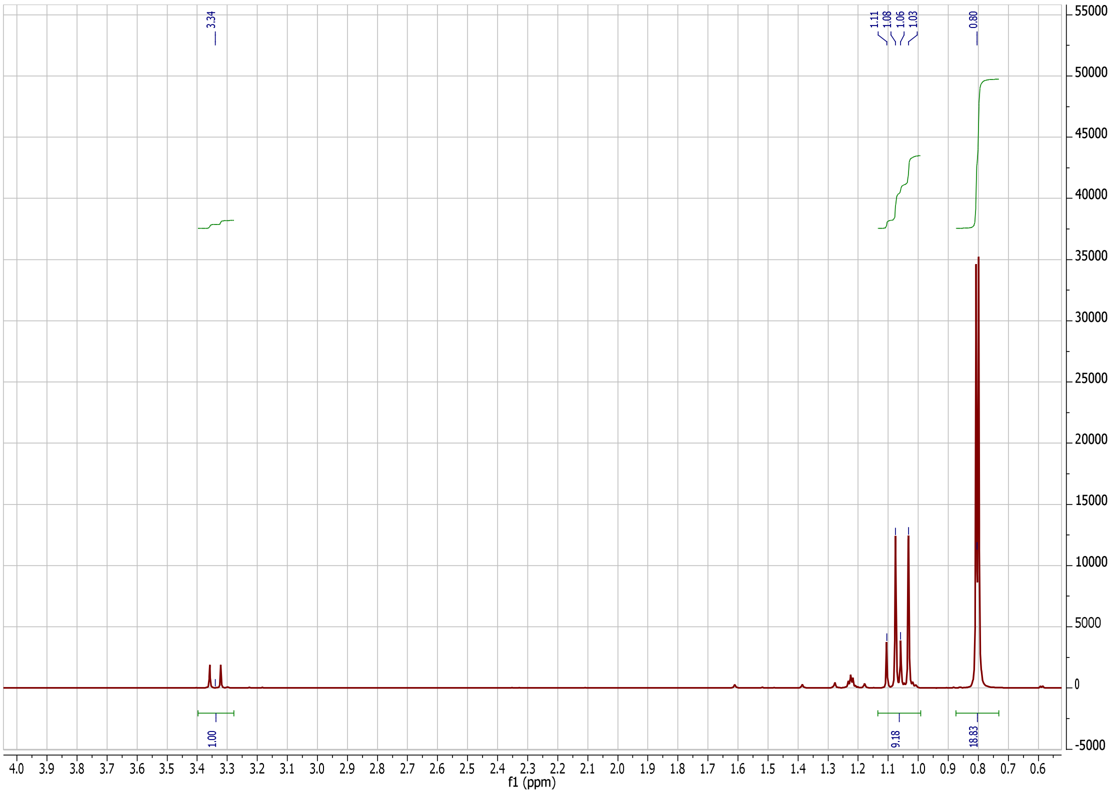

Figure S37. Proton NMR resonances of the catalytic aerobic oxidation of PMe_3 using 1 mol% of **2** under O_2 pressure (1.5 atm) in C_6D_6 at ambient conditions after t=24h; Depicted integrals correspond to the ratio of products ($OP(OMe)Me_2$ and $OPMe_3$) to educt (PMe_3).

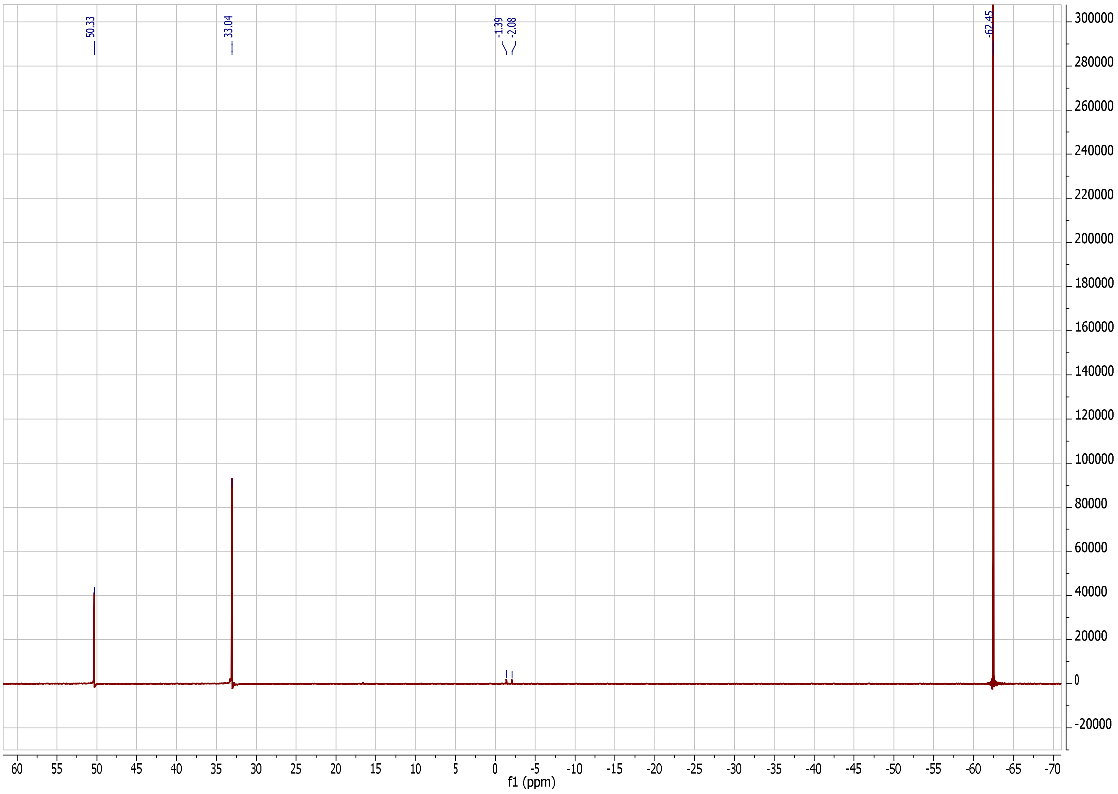

Figure S38. Phosphorus NMR resonances of the catalytic aerobic oxidation of PMe_3 using 1 mol% of **2** under O_2 pressure (1.5 atm) in C_6D_6 at ambient conditions after t=24h;

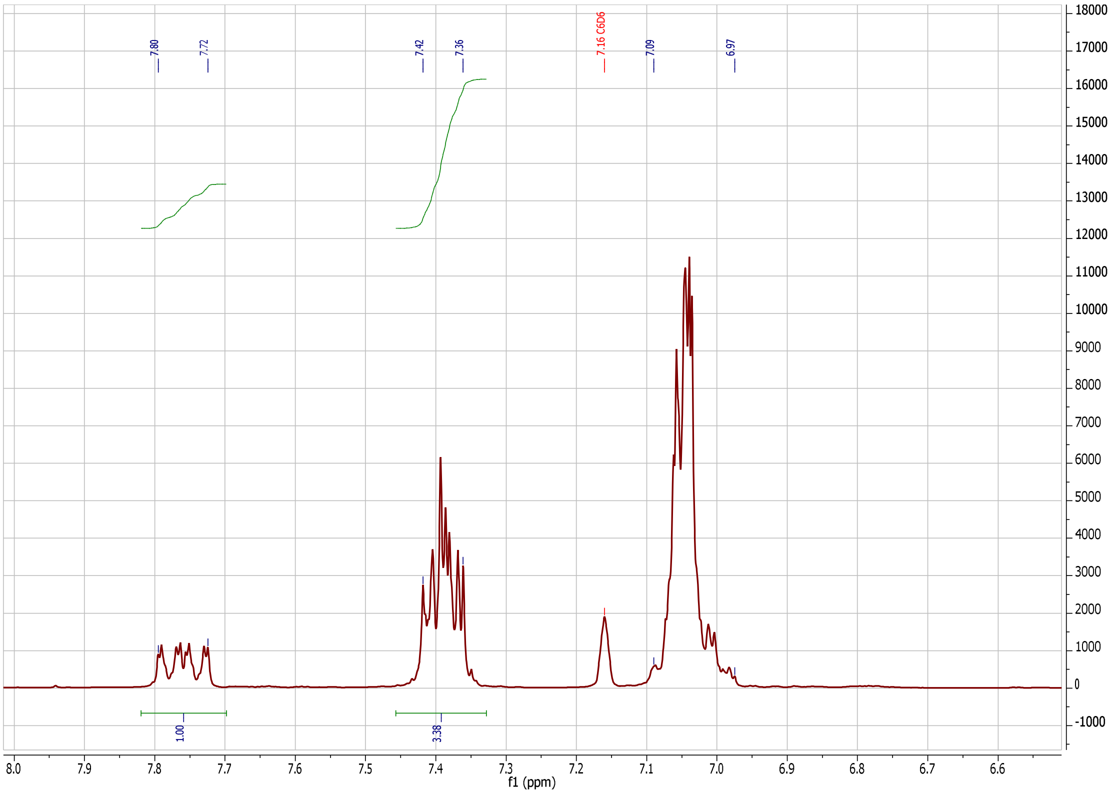

Figure S39. Proton NMR resonances of the catalytic aerobic oxidation of PPh_3 using 1 mol% of **2** under O_2 pressure (1.5 atm) in C_6D_6 at ambient conditions after t=24h; Depicted integrals correspond to the ratio of $OPPh_3$:PPh_3.

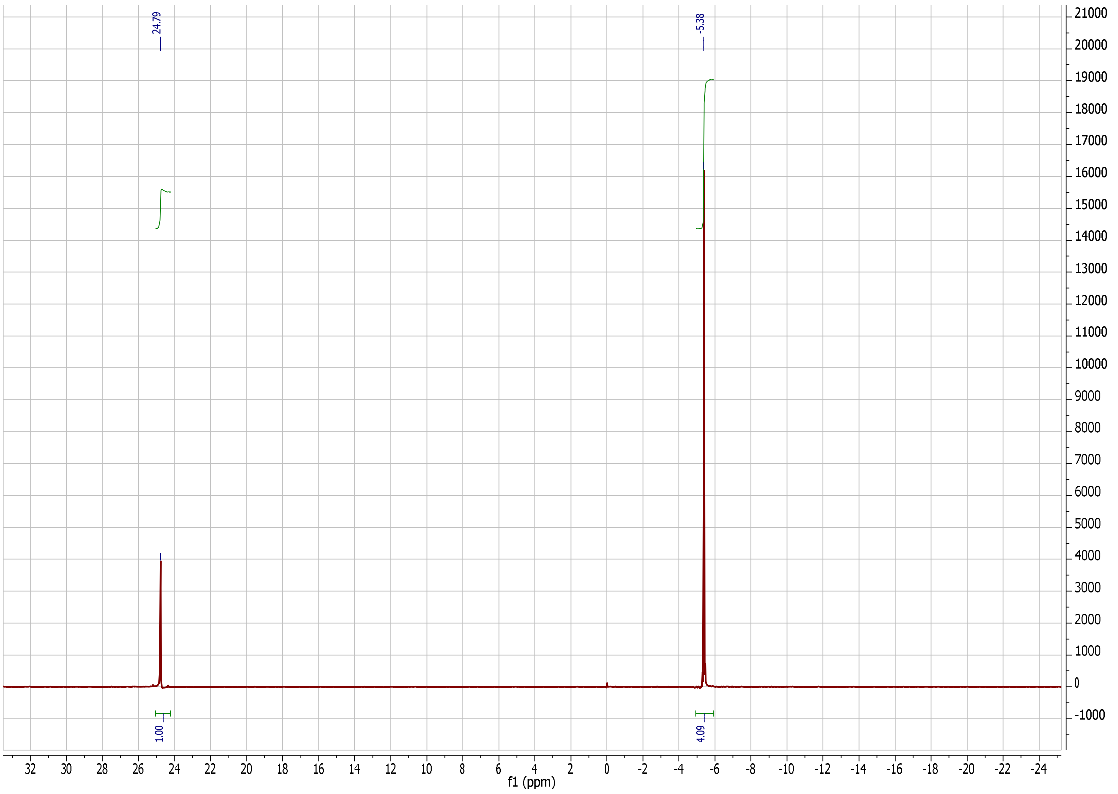

Figure S40. Phosphorus NMR resonances of the catalytic aerobic oxidation of PPh_3 using 1 mol% of **2** under O_2 pressure (1.5 atm) in C_6D_6 at ambient conditions after t=24h;

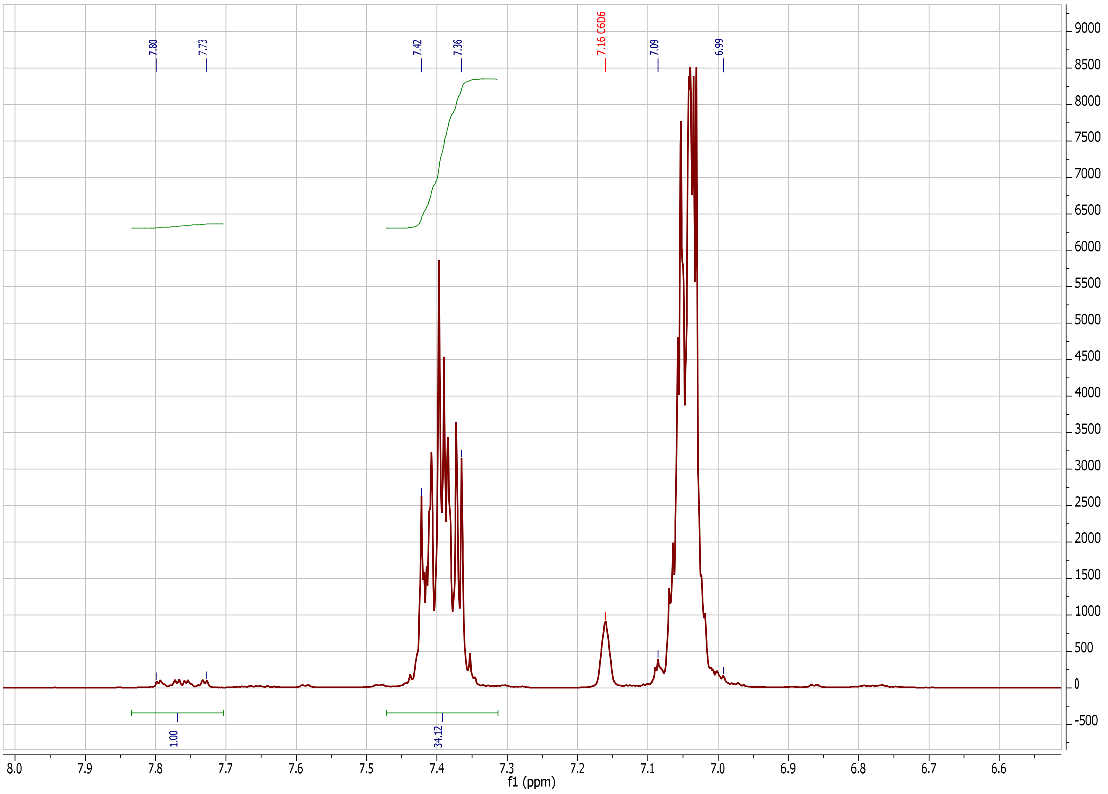

Figure S41. Proton NMR resonances of the catalytic aerobic oxidation of PPh_3 using 1 mol% of **6** under O_2 pressure (1.5 atm) in C_6D_6 at ambient conditions after t=24h; Depicted integrals correspond to the ratio of $OPPh_3$:PPh_3.

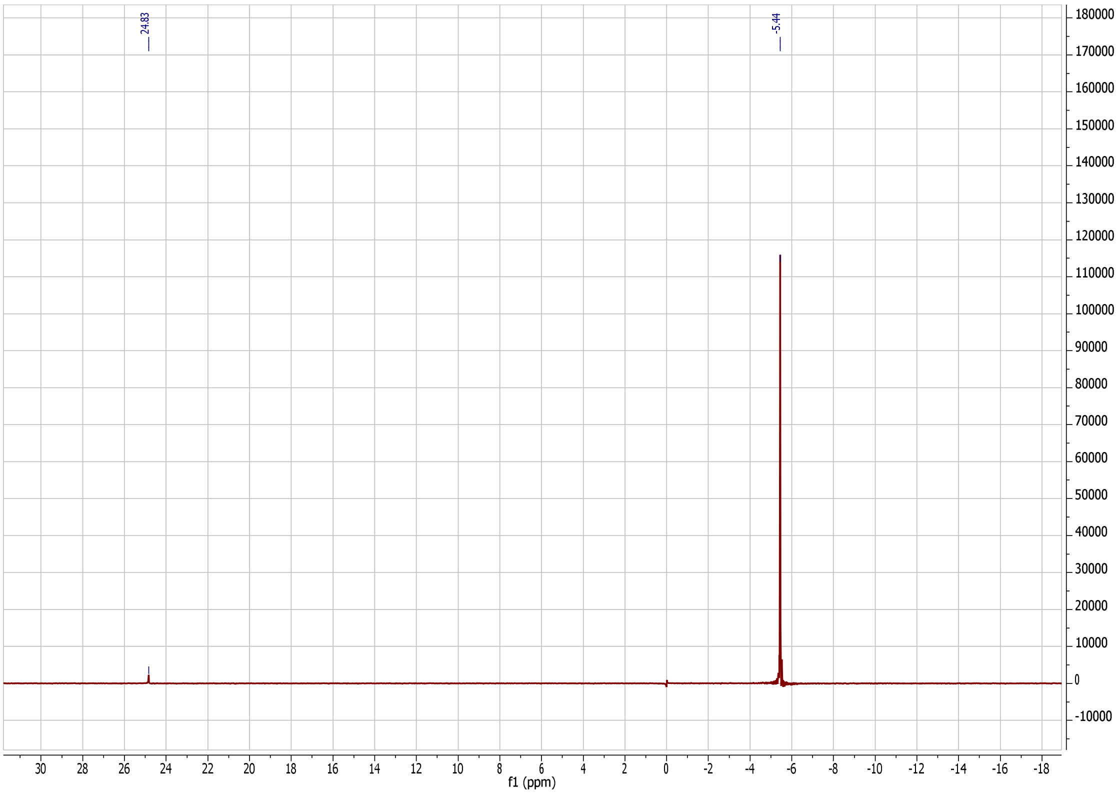

Figure S42. Phosphorus NMR resonances of the catalytic aerobic oxidation of PPh_3 using 1 mol% of **6** under O_2 pressure (1.5 atm) in C_6D_6 at ambient conditions after t=24h;

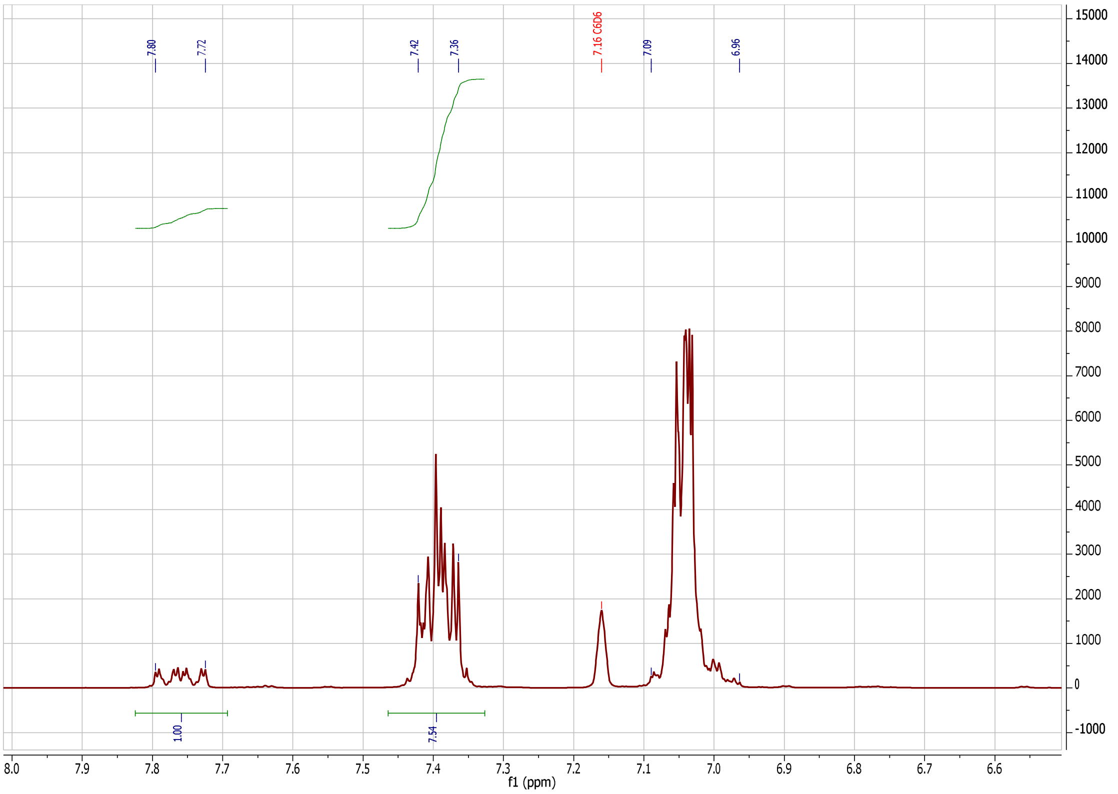

Figure S43. Proton NMR resonances of the catalytic aerobic oxidation of PPh_3 using 1 mol% of **7** under O_2 pressure (1.5 atm) in C_6D_6 at ambient conditions after t=24h; Depicted integrals correspond to the ratio of $OPPh_3$:PPh_3.

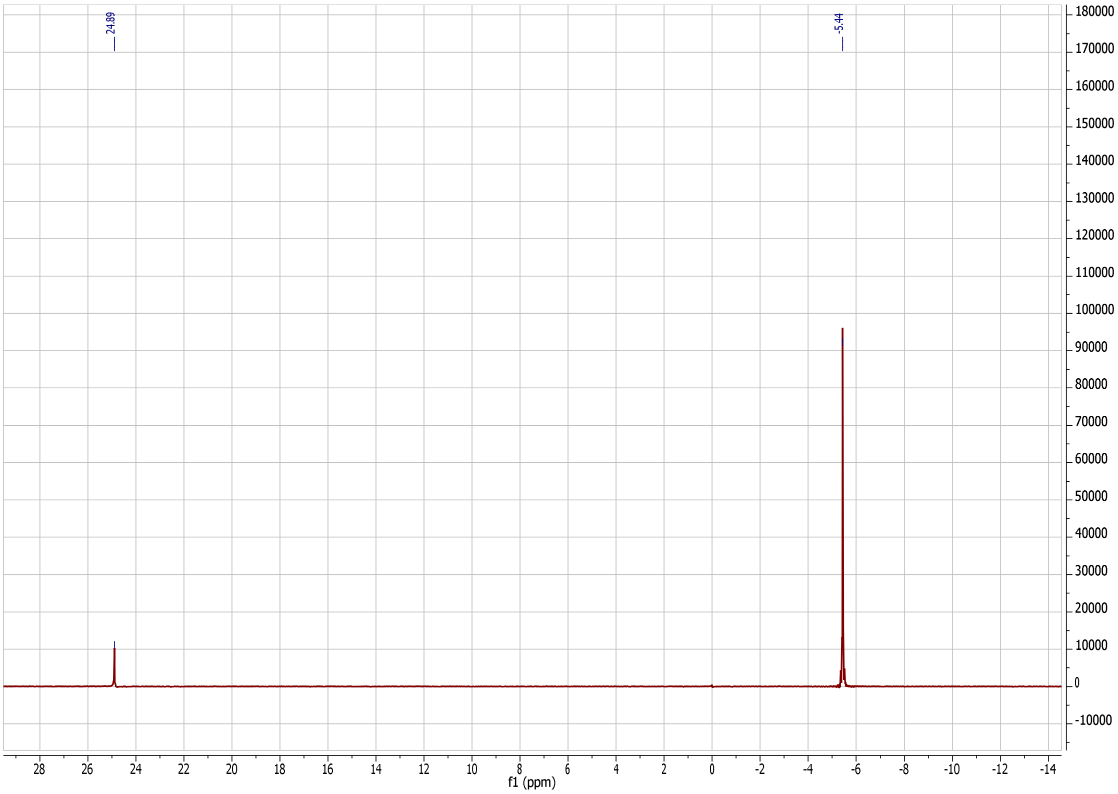

Figure S44. Phosphorus NMR resonances of the catalytic aerobic oxidation of PPh_3 using 1 mol% of **7** under O_2 pressure (1.5 atm) in C_6D_6 at ambient conditions after t=24h;

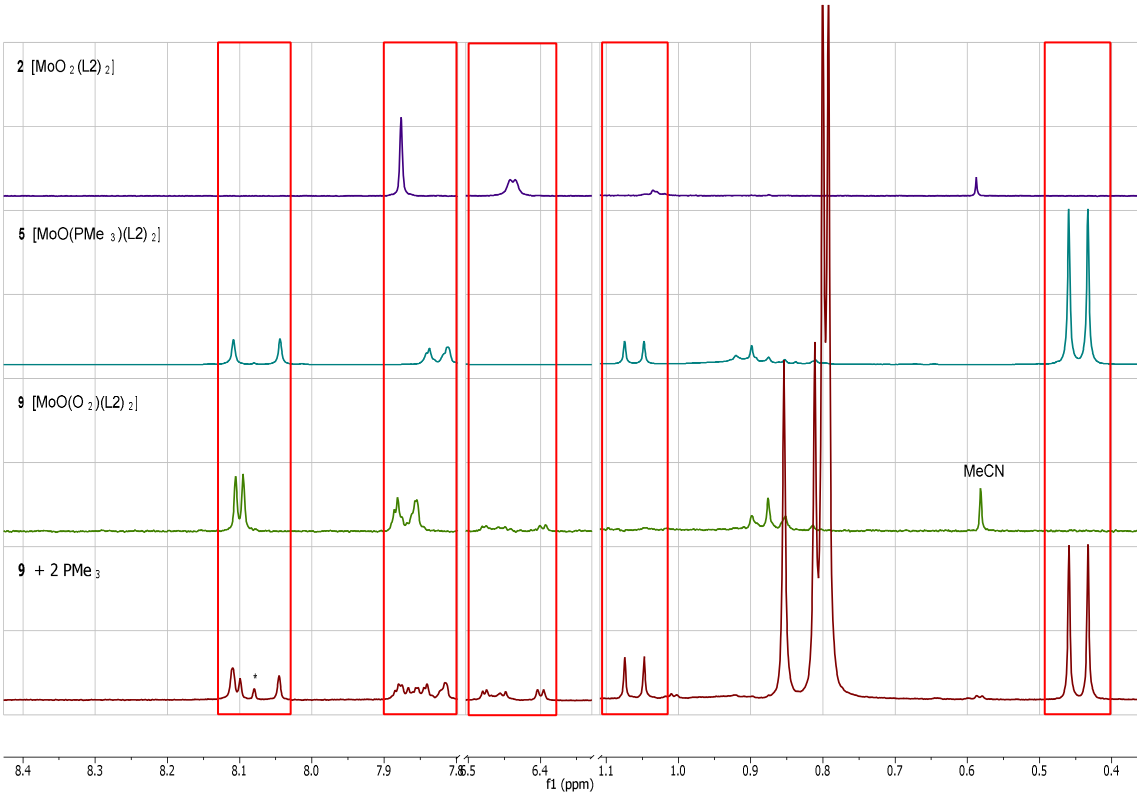

Figure S45. Selected Proton NMR resonances of a reaction of **9** [MoO(O_2)(L2)$_2$] with 2 equiv of PMe_3 after t=6h showing a mixture of **5** [MoO(PMe_3)(L2)$_2$] and compound **9** (two isomers each) but no observable amount of **2** [MoO_2(L2)$_2$].

Table S1. Selected crystallographic data and structure refinement for **1-3**, **5**, **6**, **8** and **9**.

	1	**2**	**3**	**5**	**6**	**8**	**9**
Empirical formula	$C_{38}H_{60}MoN_2O_6$	$C_{42}H_{52}MoN_2O_4 \cdot 2C_2H_3N$	$C_{26}H_{33}MoNO_5$	$C_{45}H_{61}MoN_2O_3P \cdot 2\,C_2H_3N$	$C_{76}H_{120}Mo_2N_4O_{11} \cdot 2C_2H_3N$	$C_{38}H_{60}MoN_2O_7$	$C_{42}H_{52}MoN_2O_5 \cdot C_2H_3N$
Formula weight	736.82	826.90	535.47	886.97	1539.74	752.82	801.85
Crystal description	block, yellow	block, yellow	needle, yellow	block, red	hexag.prism, red	block, red	block, orange
Crystal size	0.21x0.18x0.10mm	0.28x0.14x0.09mm	0.35x0.27x0.22mm	0.33x0.30x0.26mm	0.21x0.21x0.10mm	0.30x0.26x0.25mm	0.33x0.22x0.17mm
Crystal system, space group	monoclinic, P 2/c	triclinic, P -1	triclinic, P -1	monoclinic, C c	hexagonal, P 6_2	triclinic, P -1	triclinic, P -1
a [Å]	15.2606(7)	15.4021(18)	12.1713(10)	24.303(3)	20.8493(5)	12.7072(6)	11.644(3)
b [Å]	6.7476(3)	15.8934(17)	19.2747(15)	11.8823(17)	20.8493(5)	13.9605(6)	13.947(3)
c [Å]	19.2173(9)	18.927(2)	23.7171(19)	20.158(3)	17.0636(6)	14.0637(7)	14.644(4)
α [°]		82.417(6)	109.3961(15)			109.1480(19)	107.150(5)
β [°]	96.6167(18)	81.517(5)	91.7499(16)	123.096(2)		113.2260(18)	104.487(6)
γ [°]		75.416(5)	101.7046(15)			103.9996(16)	98.883(6)
Volume [Å^3]	1965.67(16)	4413.0(9)	5110.1(7)	4876.8(12)	6423.7(4)	1957.78(16)	2132.3(9)
Z	2	4	8	4	3	2	2
Unit cell determination	2.39° <Θ< 30.95°	2.38°<Θ<26.84°	2.75°<Θ<35.61°	2.67°<Θ< 35.63°	2.55°<Θ<28.51°	2.49°<Θ<30.80°	2.64°<Θ<30.68°
Reflections used	8005	9939	9881	9401	9536	9949	9822
Θ range for data collection	2.13 to 29.99°	1.83 to 26.00°	1.96 to 30.00°	2.41 to 35.00°	2.55 to 25.00°	1.96 to 30.00°	2.51 to 30.00°
Refl. collected / unique	16638 / 5729	57224 / 17329	139145 / 29772	61113 / 20807	41606/7534	22914 / 11283	57870 / 12427
R(int), R(sigma)	0.0281, 0.0350	0.0292, 0.0695	0.0482, 0.0370	0.0261, 0.0303	0.0969, 0.0981	0.0187, 0.0236	0.0568, 0.0479
Completeness (Θ_{max})	99.7 % (29.99°)	99.9% (26.0°)	99.9% (30.0°)	100.0% (35.0°)	99.9%(25.0°)	98.8%(30.0°)	99.9%(30.0°)
Data/parameters/restraints	5729/269/16	17329 / 1069 / 8	29772/1269/0	20807 / 584 / 2	7534/497/19	11283/499/0	12427/546/17
Signif. unique refl. [$I > 2\sigma(I)$]	5160	12216	20808	19931	5744	10468	10530
Goodness-of-fit on F^2	1.066	1.132	1.018	1.049	1.034	1.131	1.044
Final R indices [$I > 2\sigma(I)$] R1, wR2	0.0313, 0.0746	0.0607, 0.1276	0.0336, 0.0887	0.0257, 0.0622	0.0547, 0.1090	0.0372, 0.0829	0.0368, 0.0791
R indices (all data) R1, wR2	0.0368, 0.0772	0.0893, 0.1375	0.0534, 0.0980	0.0281, 0.0635	0.0885, 0.1272	0.0412, 0.0853	0.0503, 0.0854
Largest Δ/σ in last cycle	0.001	0.002	0.003	0.001	0.007	0.002	0.002
Larg. difference peak and hole [e/Å^3]	0.493 and -0.485	0.770 and -0.991	1.115 and -0.854	0.763 and -0.322	0.842 and -1.196	2.058 and -2.513	0.755 and -0.994
CCDC - Number	1476035	1476036	1476037	1476038	1486756	1476039	1476040
Weighting scheme	$w=1/[\sigma^2(F_o^2)+(aP)^2+bP]$ where $P=(F_o^2+2F_c^2)/3$						

Structure determination of 1. All the measurements were performed using graphite-monochromatized Mo K_α radiation at 100K: $C_{38}H_{60}MoN_2O_6$, M_r 736.82, monoclinic, space group P 2/c, a = 15.2606(7)Å, b = 6.7476(3)Å, c = 19.2173(9)Å, β = 96.6167(18)°, V = 1965.67(16)Å^3, Z = 2, d_{calc} = 1.245g cm^{-3}, μ = 0.377mm^{-1}. A total of 16638 reflections were collected (Θ_{max} = 29.9°), from which 5729 were unique (R_{int} = 0.0281), with 5160 having $I > 2\sigma(I)$. The structure could not be solved by direct methods (SHELXS-97)[1] in P 2/c, but in the non-centrosymmetric space group P c. After completion of the molecule a two-fold rotation axis could be detected. Refinement by full-matrix least-squares techniques against F^2 (SHELXL-2014/6)[1] was performed in the centric space group P 2/c after an appropriate shift of the origin. The *tert*. butyl groups bonded to the phenyl rings are disordered over two orientations and refined with site occupation factors of 0.514(3) and 0.486(3), respectively. The C–C bonds in these groups were restrained to 1.53Å, and the same anisotropic displacement parameters were used for these disordered atoms whose positions are close together. The H atoms of the *tert*. butyl groups were included with idealized geometries with tetrahedral angles and C–H distances of 0.98Å, but enabling rotation around the C–C bond, with their isotropic displacement parameters fixed to 1.2 times U_{eq} of the C atom they are bonded to. The other non-hydrogen atoms were refined with anisotropic displacement parameters without any constraints. The H atoms of the CH_2 groups were refined with common isotropic displacement parameters for the H atoms of the same group and idealized geometry with approximately tetrahedral angles and C–H distances of 0.99Å. The H atoms of the phenyl ring were put at the external bisectors of the C–C–C angles at C–H distances of 0.95Å and common isotropic displacement parameters were refined for these H atoms. The H atom H17 was put at the external bisector of the N-C–C angle at a C–H distance of 0.95Å but the individual isotropic displacement parameter was free to refine. The H atoms of the methyl group C104 were refined with a common isotropic displacement parameter and idealized geometries with tetrahedral angles, enabling rotation around the O-C bond, and C–H distances of 0.98Å. For 269 parameters final *R* indices of R1 = 0.0313 and wR^2 = 0.0772 (GOF = 1.066) were obtained. The largest peak in a difference Fourier map was 0.493eÅ^{-3}.

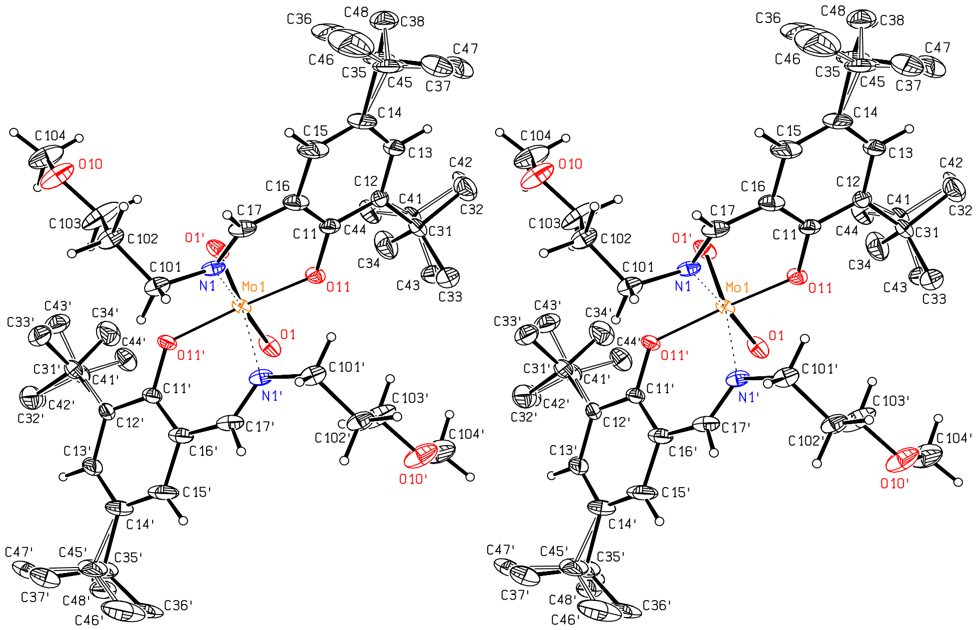

Figure S46. Stereoscopic ORTEP[2] plot of **1** showing the atomic numbering scheme. The probability ellipsoids are drawn at the 50% probability level. The H atoms are drawn with arbitrary radii. The bonds of the disordered *tert*-butyl groups in the less occupied orientations are plotted with open bonds. The H atoms of these groups were omitted for clarity reasons.

Table S2. Additional crystal data and structure refinement for **1**.

Crystal data	
Calculated density	1.245Mg/m^3
F(000)	784
Linear absorption coefficient μ	0.377mm^{-1}
Absorption correction	semi–empirical from equivalents
Max. and min. transmission	1.000 and 0.792
Data collection	
Temperature	100K
Diffractometer	Bruker APEX–II CCD
Radiation source	fine-focus sealed tube

Radiation and wavelength	Mo K_{α}, 0.71073Å
Monochromator	graphite
Scan type	ϕ and ω scans

Refinement

Refinement method	Full-matrix least-squares on F^2
Extinction expression	none
Structure Solution Program	SHELXS–97 (Sheldrick, 2008)
Structure Refinement Program	SHELXL–2014/6 (Sheldrick, 2008)

Table S3. Selected bond lengths [Å] and angles [°] for **1**.

Mo(1)-O(1)	1.7099(11)
Mo(1)-O(11)	1.9729(11)
Mo(1)-N(1)	2.3319(12)
O(11)-C(11)	1.3469(17)
C(17)-N(1)	1.286(2)
N(1)-C(101)	1.487(2)
O(1)-Mo(1)-N(1)	163.34(5)
O(11)-Mo(1)-O(11)$^{i)}$	161.05(6)
O(1)-Mo(1)-O(1)$^{i)}$	107.83(8)
N(1)-Mo(1)-N(1)$^{i)}$	75.13(6)
C(11)-O(11)-Mo(1)	132.06(10)
N(1)-C(17)-C(16)	126.38(15)
C(17)-N(1)-C(101)	115.02(13)
C(17)-N(1)-Mo(1)	123.18(11)
C(101)-N(1)-Mo(1)	121.79(10)

Symmetry transformations used to generate equivalent atoms:

$^{i)}$ 1-x, y, 3/2-z

Structure determination of 2. All the measurements were performed using monochromatized Mo K_α radiation at 100K: $C_{42}H_{52}MoN_2O_4 \cdot 2C_2H_3N$, M_r 826.90, triclinic, space group P -1, a = 15.4021(18)Å, b = 15.8934(17)Å, c = 18.927(2)Å, α = 82.417(6)°, β = 81.517(5)°, γ = 75.416(5)°, V = 4413.0(9)Å^3, Z = 4, d_{calc} = 1.245g cm^{-3}, μ = 0.342mm^{-1}. A total of 57224 reflections were collected (Θ_{max} = 26.0°), from which 17329 were unique (R_{int} = 0.0438), with 12216 having $I > 2\sigma(I)$. The structure was solved by direct methods (SHELXS-97)[1] and refined by full-matrix least-squares techniques against F^2 (SHELXL-2014/6)[1]. The asymmetric unit consists of two formula units. Two of the four acetonitrile solvent molecules lying around a center of symmetry are disordered over two orientations each and were refined with site occupation factors of 0.613(5) and 0.387(5). The C–N bonds and the C–C bonds in these disordered solvent molecules were restrained to 1.14 and 1.45Å, respectively. The other non-hydrogen atoms were refined with anisotropic displacement parameters without any constraints. The H atoms of the phenyl rings were put at the external bisectors of the C–C–C angles at C–H distances of 0.95Å and common isotropic displacement parameters were refined for the H atoms of the same ring. The H atoms of the N=CH double bonds were put at the external bisectors of the N–C–C angles at C–H distances of 0.95Å. The isotropic displacement parameters were defined together with those of the adjacent rings. The H atoms of the *tert*-butyl groups were refined with common isotropic displacement parameters for the H atoms of the same group and idealized geometry with tetrahedral angles, staggered conformation, and C–H distances of 0.98Å. The H atoms of the methyl groups of the solvent molecules were refined with one common isotropic displacement parameter and idealized geometries with tetrahedral angles, enabling rotation around the C–C bond, and C–H distances of 0.98Å. For 1069 parameters final *R* indices of R1 = 0.0607 and wR^2 = 0.1375 (GOF = 1.132) were obtained. The largest peak in a difference Fourier map was 0.770eÅ^{-3}.

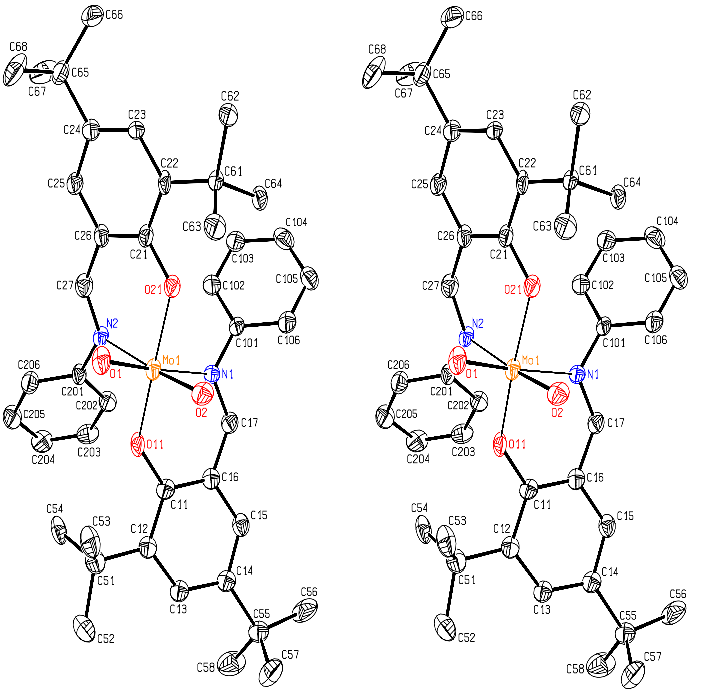

Figure S47. Stereoscopic ORTEP[2] plot of of molecule **A** of **2** showing the atomic numbering scheme. The probability ellipsoids are drawn at the 50% probability level. The H atoms were omitted for clarity reasons.

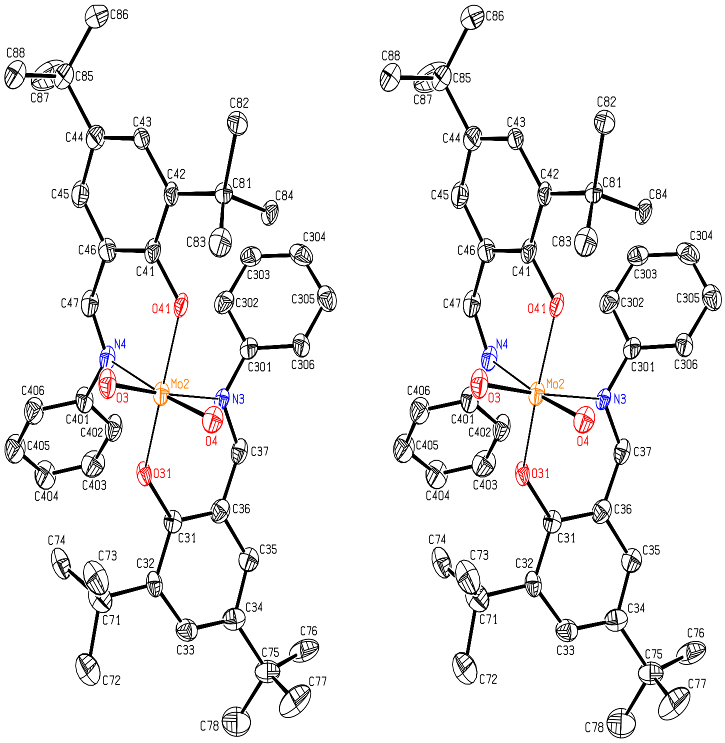

Figure S48. Stereoscopic ORTEP[2] plot of of molecule **B** of **2** showing the atomic numbering scheme. The probability ellipsoids are drawn at the 50% probability level. The H atoms were omitted for clarity reasons.

Table S4. Additional crystal data and structure refinement for **2.**

Crystal data	
Calculated density	1.245Mg/m^3
F(000)	1744
Linear absorption coefficient μ	0.342mm^{-1}
Absorption correction	semi–empirical from equivalents
Max. and min. transmission	1.000 and 0.695
Data collection	
Temperature	100K
Diffractometer	Bruker APEX–II CCD
Radiation source	Incoatec microfocus sealed tube
Radiation and wavelength	MoK$_\alpha$, 0.71073Å
Monochromator	multilayer monochromator
Scan type	ϕ and ω scans
Index ranges	$-18 \le h \le 18$, $-19 \le k \le 19$, $-23 \le l \le 23$
Refinement	
Refinement method	Full–matrix least–squares on F^2
Extinction expression	none
Structure Solution Program	SHELXS–97 (Sheldrick, 2008)
Structure Refinement Program	SHELXL–2014/6 (Sheldrick, 2008)

Table S5. Selected bond lengths [Å] and angles [°] for **2**.

Mo(1)-O(2)	1.706(3)	Mo(2)-O(3)	1.707(3)
Mo(1)-O(1)	1.707(3)	Mo(2)-O(4)	1.712(3)
Mo(1)-O(21)	1.946(2)	Mo(2)-O(41)	1.943(2)
Mo(1)-O(11)	1.946(3)	Mo(2)-O(31)	1.946(2)
Mo(1)-N(1)	2.375(3)	Mo(2)-N(3)	2.375(3)
Mo(1)-N(2)	2.394(3)	Mo(2)-N(4)	2.383(3)
O(11)-C(11)	1.328(4)	O(31)-C(31)	1.338(4)
C(17)-N(1)	1.279(5)	C(37)-N(3)	1.292(4)
N(1)-C(101)	1.434(4)	N(3)-C(301)	1.425(5)
O(21)-C(21)	1.344(4)	O(41)-C(41)	1.361(4)
C(27)-N(2)	1.283(5)	C(47)-N(4)	1.294(5)
N(2)-C(201)	1.423(4)	N(4)-C(401)	1.454(5)
O(21)-Mo(1)-O(11)	152.33(11)	C(201)-N(2)-Mo(1)	122.6(2)
O(1)-Mo(1)-N(1)	169.84(12)	O(41)-Mo(2)-O(31)	152.37(11)
O(2)-Mo(1)-N(2)	168.57(12)	O(3)-Mo(2)-N(3)	169.75(11)
C(11)-O(11)-Mo(1)	131.3(2)	O(4)-Mo(2)-N(4)	168.09(12)
N(1)-C(17)-C(16)	127.6(4)	C(31)-O(31)-Mo(2)	131.9(2)
C(17)-N(1)-C(101)	115.8(3)	N(3)-C(37)-C(36)	128.2(4)
C(17)-N(1)-Mo(1)	117.6(3)	C(37)-N(3)-C(301)	115.4(3)
C(101)-N(1)-Mo(1)	124.3(2)	C(37)-N(3)-Mo(2)	118.7(2)
C(21)-O(21)-Mo(1)	133.2(2)	C(301)-N(3)-Mo(2)	123.7(2)
N(2)-C(27)-C(26)	127.2(4)	C(41)-O(41)-Mo(2)	132.6(2)
C(27)-N(2)-C(201)	116.5(3)	N(4)-C(47)-C(46)	126.4(4)
C(27)-N(2)-Mo(1)	119.1(3)	C(47)-N(4)-C(401)	115.5(3)

C(47)-N(4)-Mo(2)	120.9(3)
C(401)-N(4)-Mo(2)	121.9(2)
Mo(1)-O(11)-C(11)-C(12)	142.5(3)
C(16)-C(17)-N(1)-C(101)	-177.3(4)
C(16)-C(17)-N(1)-Mo(1)	19.2(5)
C(17)-N(1)-C(101)-C(102)	133.1(4)
Mo(1)-O(21)-C(21)-C(22)	144.5(3)
C(26)-C(27)-N(2)-C(201)	-177.0(4)
C(26)-C(27)-N(2)-Mo(1)	17.8(5)
C(27)-N(2)-C(201)-C(202)	125.4(4)
Mo(2)-O(31)-C(31)-C(32)	142.4(3)
C(36)-C(37)-N(3)-C(301)	-179.6(4)
C(36)-C(37)-N(3)-Mo(2)	17.0(5)
C(37)-N(3)-C(301)-C(302)	130.8(4)
Mo(2)-O(41)-C(41)-C(42)	141.8(3)
C(46)-C(47)-N(4)-C(401)	-178.6(4)
C(46)-C(47)-N(4)-Mo(2)	16.0(5)
C(47)-N(4)-C(401)-C(402)	122.8(4)

Structure determination of 3. All the measurements were performed using monochromatized Mo K_α radiation at 100K: $C_{26}H_{33}MoNO_5$, M_r 535.47, triclinic, space group P -1, a = 12.1713(10)Å, b = 19.2747(15)Å, c = 23.7171(19)Å, α = 109.3961(15)°, β = 91.7499(16)°, γ = 101.7046(15)°, V = 5110.1(7)$Å^3$, Z = 8, d_{calc} = 1.392g cm^{-3}, μ = 0.548mm^{-1}. A total of 139145 reflections were collected (Θ_{max} = 30.0°), from which 29772 were unique (R_{int} = 0.0482), with 20808 having $I > 2\sigma(I)$. The structure was solved by direct methods (SHELXS-97)[1] and refined by full-matrix least-squares techniques against F^2 (SHELXL-2014/6).[1] The non-hydrogen atoms were refined with anisotropic displacement parameters without any constraints. The H atoms of the phenyl rings were put at the external bisectors of the C–C–C angles at C–H distances of 0.95Å and common isotropic displacement parameters were refined for the H atoms of the same ring. The H atoms bonded to a C atom of a N=CH group or to the central C atom of an acac ligand were put at the external bisectors of the X–C–C angles at C–H distances of 0.95Å but the individual isotropic displacement parameters were free to refine. The H atoms of the methyl groups were refined with common isotropic displacement parameters for the H atoms of the same group and idealized geometries with tetrahedral angles, enabling rotation around the C–C bond, and C–H distances of 0.98Å. For 1269 parameters final *R* indices of R1 = 0.0336 and wR^2 = 0.0980 (GOF = 1.018) were obtained. The largest peak in a difference Fourier map was 1.115e$Å^{-3}$.

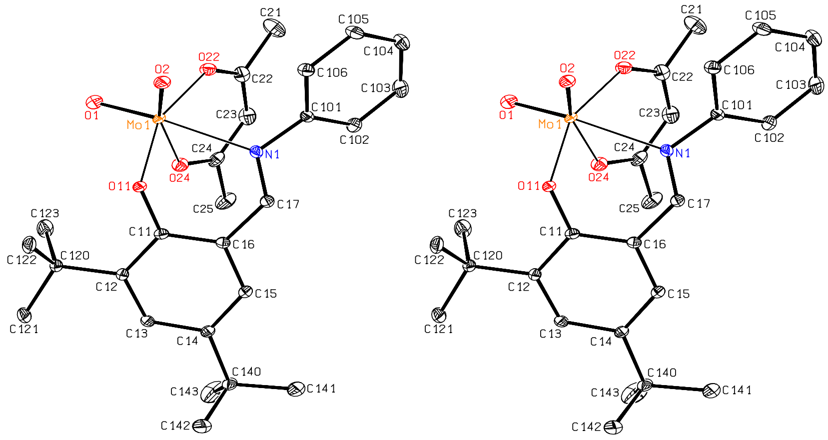

Figure S49. Stereoscopic ORTEP[2] plot of one of the four complexes of the asymmetric unit of **3** showing the atomic numbering scheme. The probability ellipsoids are drawn at the 50% probability level. The H atoms were omitted for clarity reasons.

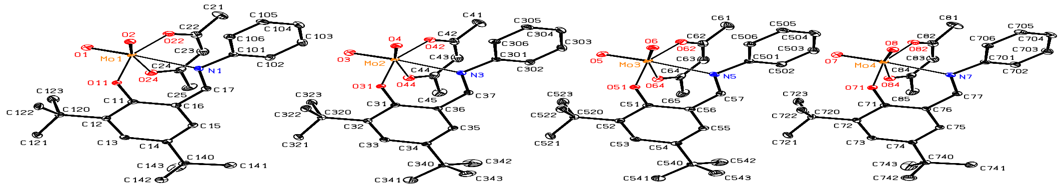

Figure S50. ORTEP[2] plot of the four complexes of the asymmetric unit of **3**. The probability ellipsoids are drawn at the 50% probability level. The H atoms were omitted for clarity reasons.

Table S6. Additional crystal data and structure refinement for **3**.

Crystal data	
Calculated density	1.392Mg/m^3
F(000)	2224
Linear absorption coefficient μ	0.548mm^{-1}
Absorption correction	semi–empirical from equivalents
Max. and min. transmission	0.747 and 0.568
Data collection	
Temperature	100K
Diffractometer	Bruker APEX–II CCD

Radiation source	fine-focus sealed tube
Radiation and wavelength	MoK$_\alpha$, 0.71073Å
Monochromator	graphite
Scan type	ϕ and ω scans
Refinement	
Refinement method	Full–matrix least–squares on F^2
Extinction expression	none
Structure Solution Program	SHELXS–97 (Sheldrick, 2008)
Structure Refinement Program	SHELXL–2014/6 (Sheldrick, 2008)

Table S7. Selected bond lengths [Å] and angles [°] for **2**.

Mo(1)-O(1)	1.7049(13)	Mo(3)-O(5)	1.7061(13)
Mo(1)-O(2)	1.7103(12)	Mo(3)-O(6)	1.7109(13)
Mo(1)-O(11)	1.9280(12)	Mo(3)-O(51)	1.9304(13)
Mo(1)-O(22)	2.0075(12)	Mo(3)-O(62)	2.0119(13)
Mo(1)-O(24)	2.1812(12)	Mo(3)-O(64)	2.1917(13)
Mo(1)-N(1)	2.4021(15)	Mo(3)-N(5)	2.3997(15)
O(11)-C(11)	1.345(2)	O(51)-C(51)	1.349(2)
C(17)-N(1)	1.290(2)	C(57)-N(5)	1.291(2)
N(1)-C(101)	1.436(2)	N(5)-C(501)	1.439(2)
C(22)-O(22)	1.300(2)	C(62)-O(62)	1.306(2)
C(24)-O(24)	1.259(2)	C(64)-O(64)	1.261(2)
Mo(2)-O(3)	1.7097(13)	Mo(4)-O(7)	1.7089(13)
Mo(2)-O(4)	1.7028(13)	Mo(4)-O(8)	1.7106(12)
Mo(2)-O(31)	1.9276(12)	Mo(4)-O(71)	1.9243(12)
Mo(2)-O(42)	2.0110(12)	Mo(4)-O(82)	2.0135(12)
Mo(2)-O(44)	2.1926(12)	Mo(4)-O(84)	2.1888(12)
Mo(2)-N(3)	2.3992(15)	Mo(4)-N(7)	2.3974(15)
O(31)-C(31)	1.348(2)	O(71)-C(71)	1.346(2)
C(37)-N(3)	1.291(2)	C(77)-N(7)	1.293(2)
N(3)-C(301)	1.439(2)	N(7)-C(701)	1.436(2)
C(42)-O(42)	1.302(2)	C(82)-O(82)	1.302(2)
C(44)-O(44)	1.258(2)	C(84)-O(84)	1.256(2)

O(1)-Mo(1)-N(1)	167.95(6)	C(42)-O(42)-Mo(2)	134.63(12)
O(2)-Mo(1)-O(24)	163.75(6)	C(44)-O(44)-Mo(2)	131.61(12)
O(11)-Mo(1)-O(22)	153.88(5)	O(5)-Mo(3)-N(5)	167.05(6)
C(11)-O(11)-Mo(1)	132.56(11)	O(6)-Mo(3)-O(64)	165.13(6)
C(17)-N(1)-C(101)	117.38(15)	O(51)-Mo(3)-O(62)	153.06(5)
C(17)-N(1)-Mo(1)	122.86(11)	C(51)-O(51)-Mo(3)	131.57(11)
C(101)-N(1)-Mo(1)	119.51(11)	C(57)-N(5)-C(501)	117.76(15)
C(22)-O(22)-Mo(1)	134.63(12)	C(57)-N(5)-Mo(3)	122.30(11)
C(24)-O(24)-Mo(1)	131.36(12)	C(501)-N(5)-Mo(3)	119.56(11)
O(3)-Mo(2)-N(3)	166.96(6)	C(62)-O(62)-Mo(3)	134.74(13)
O(4)-Mo(2)-O(44)	164.97(6)	C(64)-O(64)-Mo(3)	131.91(12)
O(31)-Mo(2)-O(42)	153.30(5)	O(7)-Mo(4)-N(7)	167.78(6)
C(31)-O(31)-Mo(2)	132.10(11)	O(8)-Mo(4)-O(84)	164.22(6)
C(37)-N(3)-C(301)	117.55(15)	O(71)-Mo(4)-O(82)	153.74(5)
C(37)-N(3)-Mo(2)	122.75(11)	C(71)-O(71)-Mo(4)	132.13(11)
C(301)-N(3)-Mo(2)	119.30(11)	C(77)-N(7)-C(701)	117.40(15)

C(77)-N(7)-Mo(4)	122.63(11)	C(82)-O(82)-Mo(4)	134.51(12)
C(701)-N(7)-Mo(4)	119.74(11)	C(84)-O(84)-Mo(4)	131.74(11)

C(11)-C(12)-C(120)-C(121)	-175.96(16)
C(13)-C(14)-C(140)-C(141)	-175.96(15)
C(31)-C(32)-C(320)-C(321)	-174.76(15)
C(33)-C(34)-C(340)-C(341)	2.3(2)
C(51)-C(52)-C(520)-C(521)	-176.26(16)
C(53)-C(54)-C(540)-C(541)	3.1(2)
C(71)-C(72)-C(720)-C(721)	-177.72(15)
C(73)-C(74)-C(740)-C(741)	-174.73(15)

Structure determination of 5. All the measurements were performed using monochromatized Mo K_{α} radiation at 100K: $C_{45}H_{61}MoN_2O_3P \cdot 2CH_3CN$, M_r 886.97, monoclinic, space group C c, a = 24.303(3)Å, b = 11.8823(17)Å, c = 20.158(3)Å, β = 123.096(2)°, V = 4876.8(12)$Å^3$, Z = 4, d_{calc} = 1.208g cm^{-3}, μ = 0.344mm^{-1}. A total of 61113 reflections were collected (Θ_{max} = 35.0°), from which 20807 were unique (R_{int} = 0.0261), with 19931 having $I > 2\sigma(I)$. The structure was solved by direct methods (SHELXS-97)[1] and refined by full-matrix least-squares techniques against F^2 (SHELXL-2014/6).[1] The absolute configuration was established by anomalous dispersion effects in the diffraction measurements on the crystal. The non-hydrogen atoms were refined with anisotropic displacement parameters without any constraints. The *tert.* butyl group bonded to C24 was disordered over two orientations and refined with site occupation factors of 0.819(4) and 0.181(4), respectively. The H atoms of the phenyl rings as well as those of the imino groups were put at the external bisectors of the X–C–C angles at C–H distances of 0.95Å and common isotropic displacement parameters were refined for the H atoms of the same phenyl ring. The H atoms of the methyl groups and those of the *tert.* butyl groups were refined with common isotropic displacement parameters for the H atoms of the same group and idealized geometries with tetrahedral angles, enabling rotation around the C–C bond, and C–H distances of 0.98Å. The largest peaks in a final difference Fourier map (0.53 - 0.76e$Å^{-3}$) were in the vicinity (0.69 - 0.76Å) of the Mo atom. For 584 parameters final *R* indices of R1 = 0.0257 and wR^2 = 0.0635 (GOF = 1.049) were obtained.

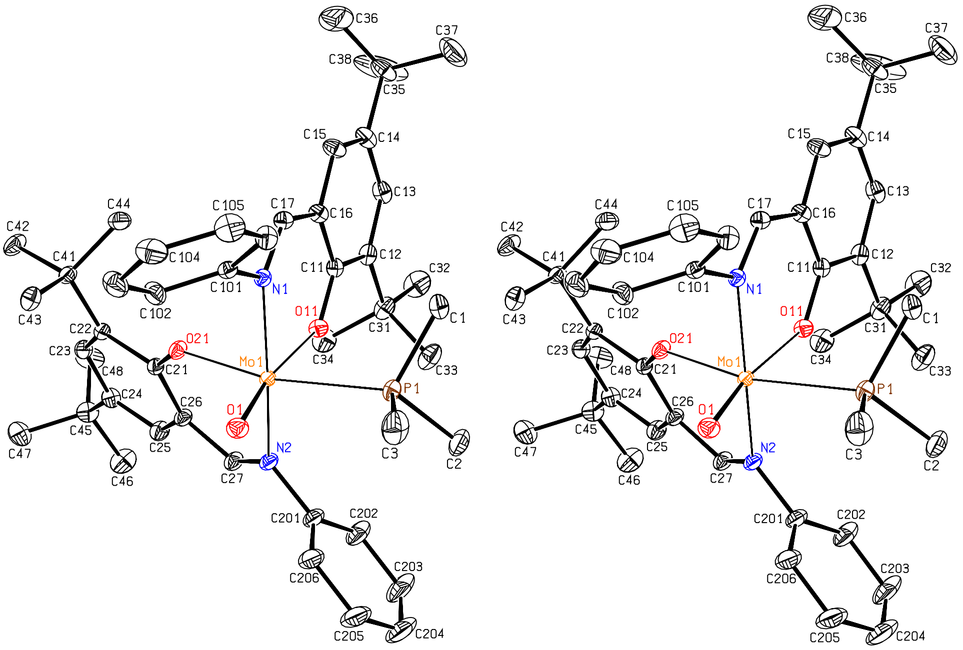

Figure S51. Stereoscopic ORTEP[2] plot of **5** showing the atomic numbering scheme. The probability ellipsoids are drawn at the 50% probability level. The H atoms, the disordered *tert.* butyl group in the orientation with a low site occupation factor of 0.181(4), and the acetonitrile solvent molecules were omitted for clarity reasons.

Table S8. Additional crystal data and structure refinement for **5**.

Crystal data	
Calculated density	1.392Mg/m^3
F(000)	2224
Linear absorption coefficient μ	0.344mm^{-1}
Absorption correction	semi–empirical from equivalents
Max. and min. transmission	0.747 and 0.676
Data collection	
Temperature	100K
Diffractometer	Bruker APEX–II CCD
Radiation source	fine-focus sealed tube
Radiation and wavelength	MoK$_\alpha$, 0.71073Å
Monochromator	graphite
Scan type	ϕ and ω scans
Refinement	
Refinement method	Full–matrix least–squares on F^2
Extinction expression	none
Structure Solution Program	SHELXS–97 (Sheldrick, 2008)
Structure Refinement Program	SHELXL–2014/6 (Sheldrick, 2008)

Table S9. Selected bond lengths [Å] and angles [°] for **5**.

Mo(1)-O(1)	1.7037(13)
Mo(1)-O(11)	2.0660(14)
Mo(1)-O(21)	2.0816(11)
Mo(1)-N(1)	2.1272(13)
Mo(1)-N(2)	2.1769(13)
Mo(1)-P(1)	2.5289(6)
P(1)-C(1)	1.824(2)
P(1)-C(2)	1.8249(18)
P(1)-C(3)	1.826(2)
C(17)-N(1)	1.309(2)
C(27)-N(2)	1.302(2)

O(1)-Mo(1)-O(11)	169.78(6)
P(1)-Mo(1)-O(21)	168.00(4)
N(1)-Mo(1)-N(2)	164.99(5)
O(1)-Mo(1)-P(1)	86.87(5)
O(11)-Mo(1)-P(1)	83.18(4)
N(1)-Mo(1)-P(1)	87.38(4)
N(2)-Mo(1)-P(1)	100.09(4)
C(1)-P(1)-C(2)	101.38(9)
C(1)-P(1)-C(3)	102.01(11)
C(2)-P(1)-C(3)	101.65(11)
C(1)-P(1)-Mo(1)	113.95(6)
C(2)-P(1)-Mo(1)	123.07(7)
C(3)-P(1)-Mo(1)	112.11(7)
C(11)-O(11)-Mo(1)	137.42(10)
C(17)-N(1)-C(101)	114.78(12)
C(17)-N(1)-Mo(1)	128.53(11)
C(101)-N(1)-Mo(1)	116.63(9)
C(21)-O(21)-Mo(1)	131.39(9)
C(27)-N(2)-C(201)	115.40(13)
C(27)-N(2)-Mo(1)	123.47(10)
C(201)-N(2)-Mo(1)	121.03(10)

Crystal structure determination of 6. All the measurements were performed using monochromatized Mo K_α radiation at 100K: $C_{76}H_{120}Mo_2N_4O_{11} \cdot 2C_2H_3N$, M_r 1539.74, hexagonal, space group P 6_2, a = 20.8493(5)Å, b = 20.8493(5)Å, c = 17.0636(6)Å, V = 6423.7(4)Å^3, Z = 3, d_{calc} = 1.194g cm^{-3}, μ = 0.349mm^{-1}. A total of 41606 reflections were collected (Θ_{max} = 25.0°), from which 7534 were unique (R_{int} = 0.0969), with 5744 having $I > 2\sigma(I)$. The structure was solved by direct methods (SHELXS-97)[2] in P 3_2. After completion of the molecule a two-fold rotation axis through the μ_2-oxo atom could be detected. Refinement by full-matrix least-squares techniques against F^2 (SHELXL-2014/6)[2] in space group P 6_2 after an appropriate shift of the origin. The absolute configuration was established by anomalous dispersion effects in the diffraction measurements on the crystal. The methoxypropyl group bonded to N2 was disordered over two orientations and refined with site occupation factors of 0.517(14) and 0.483(14), respectively. The equivalent bonds in this disordered group were restrained to have the same lengths and the same anisotropic displacement parameters were used for the two atoms C202/C212, and C203/C213 whose positions are close together. The disordered acetonitrile solvent molecules were refined as rigid bodies; their equivalent bonds were restrained to have the same lengths. The other non-hydrogen atoms were refined with anisotropic displacement parameters without any constraints. The H atoms of the phenyl rings as well as those of the imino groups were put at the external bisectors of the X–C–C angles at C–H distances of 0.95Å and common isotropic displacement parameters were refined for the H atoms of the same ligand. The H atoms of the CH_2 groups were refined with common isotropic displacement parameters for the H atoms of the same propyl group and idealized geometry with approximately tetrahedral angles and C–H distances of 0.99Å. The H atoms of the methyl groups were refined with common isotropic displacement parameters for the H atoms of the same methyl group or of the same *tert*-butyl group, resp., and idealized geometries with tetrahedral angles, enabling rotation around the X–C bond, and C–H distances of 0.98Å. For 497 parameters final *R* indices of R1 = 0.0547 and wR^2 = 0.1272 (GOF = 1.034) were obtained. The largest peak in a difference Fourier map was 0.842eÅ^{-3}.

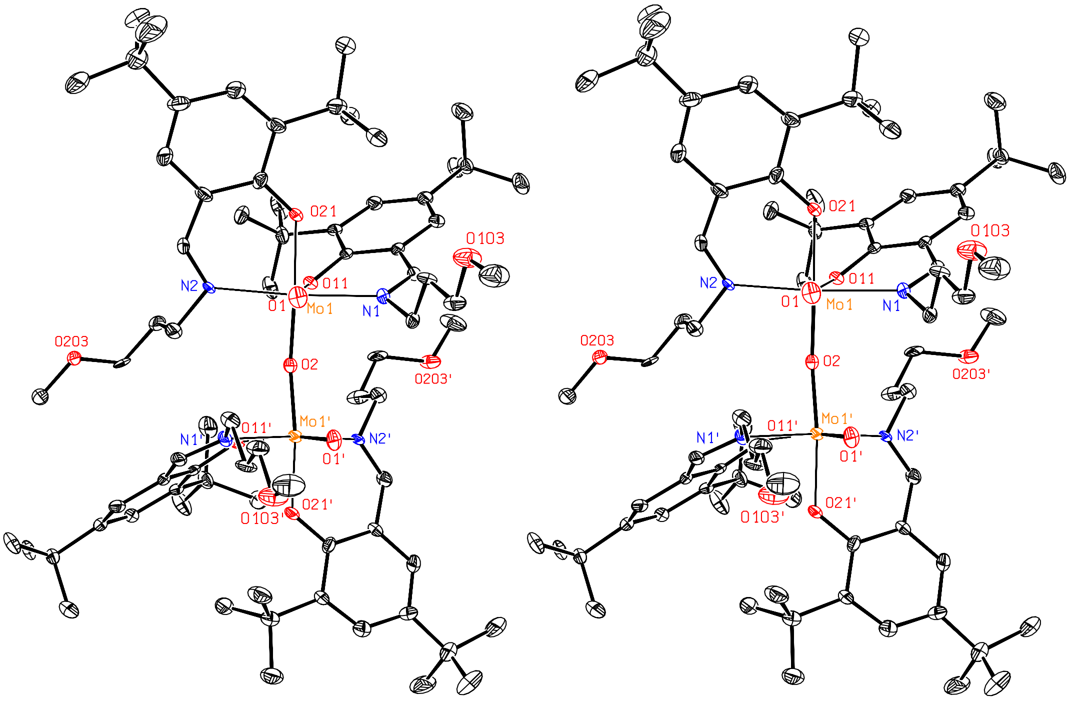

Figure S52. Stereoscopic ORTEP[2] plot of **6** showing the atomic numbering scheme. The probability ellipsoids are drawn at the 50% probability level. The H atoms as well as the less occupied disordered methoxypropyl group were omitted for clarity reasons.

Table S10. Additional crystal data and structure refinement for **6**.

Crystal data	
Calculated density	1.194Mg/m^3
F(000)	2460
Linear absorption coefficient μ	0.349mm^{-1}
Absorption correction	semi–empirical from equivalents
Max. and min. transmission	1.000 and 0.650
Data collection	
Temperature	100K
Diffractometer	Bruker APEX–II CCD

Radiation source	Incoatec microfocus sealed tube
Radiation and wavelength	MoK$_{\alpha}$, 0.71073Å
Monochromator	multilayer monochromator
Scan type	ϕ and ω scans

Refinement

Refinement method	Full–matrix least–squares on F^2
Extinction expression	none
Structure Solution Program	SHELXS–97 (Sheldrick, 2008)
Structure Refinement Program	SHELXL–2014/6 (Sheldrick, 2008)

Table S11. Selected bond lengths [Å] and angles [°] for **6**.

Mo(1)-O(1)	1.694(6)
Mo(1)-O(2)	1.8883(18)
Mo(1)-O(11)	2.054(6)
Mo(1)-O(21)	2.063(5)
Mo(1)-N(1)	2.182(6)
Mo(1)-N(2)	2.155(6)
O(11)-C(11)	1.337(9)
C(17)-N(1)	1.303(10)
O(21)-C(21)	1.311(8)
C(27)-N(2)	1.294(10)

Mo(1)-O(2)-Mo(1)$^{\mathrm{i)}}$	157.2(5)
O(1)-Mo(1)-O(11)	164.2(2)
O(2)-Mo(1)-O(21)	166.3(3)
N(1)-Mo(1)-N(2)	174.3(3)
C(11)-O(11)-Mo(1)	131.0(5)
C(17)-N(1)-C(101)	115.4(7)
C(17)-N(1)-Mo(1)	125.6(6)
C(101)-N(1)-Mo(1)	118.7(5)
C(21)-O(21)-Mo(1)	131.0(4)
C(27)-N(2)-C(201)	113.6(6)
C(27)-N(2)-Mo(1)	122.8(5)
C(201)-N(2)-Mo(1)	123.1(5)

C(16)-C(17)-N(1)-C(101)	-179.3(7)
C(16)-C(17)-N(1)-Mo(1)	-5.8(12)
C(26)-C(27)-N(2)-C(201)	-176.6(9)
C(26)-C(27)-N(2)-Mo(1)	10.9(13)

Symmetry transformation used to generate the equivalent atom:

$^{\mathrm{i)}}$ 1-x, 2-y, z

Crystal structure determination of 8. All the measurements were performed using monochromatized Mo K_α radiation at 100K: $C_{38}H_{60}MoN_2O_7$, M_r 752.82, triclinic, space group P -1, a = 12.7072(6)Å, b = 13.9605(6)Å, c = 14.0637(7)Å, α = 109.1480(19)°, β = 113.2260(18)°, γ = 103.9996(16)°, V = 1957.78(16)Å^3, Z = 2, d_{calc} = 1.277g cm^{-3}, μ = 0.382mm^{-1}. A total of 22914 reflections were collected (Θ_{max} = 30.0°), from which 11283 were unique (R_{int} = 0.0187), with 10468 having $I > 2\sigma(I)$. The structure was solved by direct methods (SHELXS-97)[1] and refined by full-matrix least-squares techniques against F^2 (SHELXL-2014/6).[1] The non-hydrogen atoms were refined with anisotropic displacement parameters without any constraints. The oxo and peroxo groups are disordered over two orientations. Site occupation factors [0.710(4) and 0.290(4), resp.] adding to unity were refined for the two orientations. The H atoms of the CH_2 groups were refined with common isotropic displacement parameters for the H atoms of the same group and idealized geometry with approximately tetrahedral angles and C–H distances of 0.99Å. The H atoms of the phenyl rings were put at the external bisectors of the C–C–C angles at C–H distances of 0.95Å and common isotropic displacement parameters were refined for the H atoms of the same phenyl group. The H atoms H17 and H27 were put at the external bisector of the C–C–C angle at a C–H distance of 0.95Å but the individual isotropic displacement parameters were free to refine. The H atoms of the methyl groups were refined with common isotropic displacement parameters for the H atoms of the same group and idealized geometries with tetrahedral angles, enabling rotation around the X–C bond, and C–H distances of 0.98Å. For 499 parameters final *R* indices of R1 = 0.0372 and wR^2 = 0.0853 (GOF = 1.131) were obtained. The largest peak in a difference Fourier map was 2.058eÅ^{-3}.

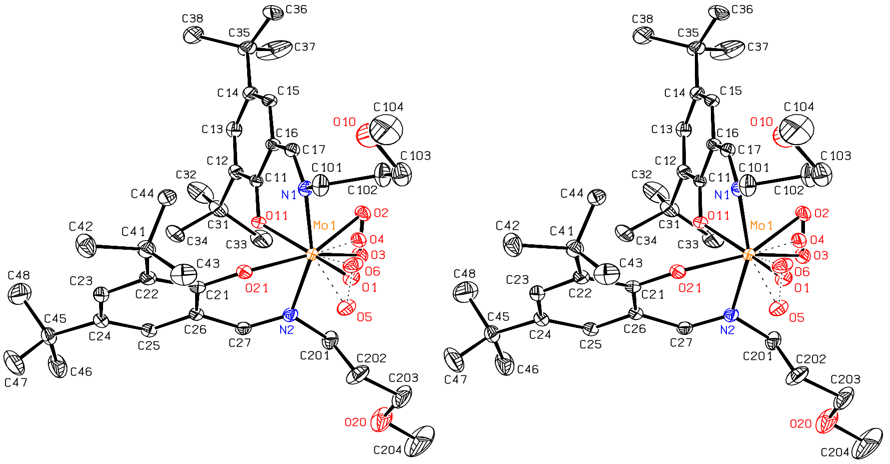

Figure S53. Stereoscopic ORTEP[2] plot of **8** showing the atomic numbering scheme. The probability ellipsoids are drawn at the 50% probability level. The H atoms were omitted for clarity reasons. The bonds to the O atoms with site occupation factors of 0.290(4) are plotted with dashed lines.

Table S12. Additional crystal data and structure refinement for **8**.

Crystal data	
Calculated density	1.277Mg/m^3
F(000)	800
Linear absorption coefficient μ	0.382mm^{-1}
Absorption correction	semi–empirical from equivalents
Max. and min. transmission	0.746 and 0.640
Data collection	
Temperature	100K
Diffractometer	Bruker APEX–II CCD
Radiation source	fine-focus sealed tube
Radiation and wavelength	MoK$_\alpha$, 0.71073Å
Monochromator	graphite
Scan type	ϕ and ω scans
Refinement	
Refinement method	Full–matrix least–squares on F^2
Extinction expression	none
Structure Solution Program	SHELXS–97 (Sheldrick, 2008)
Structure Refinement Program	SHELXL–2014/6 (Sheldrick, 2008)

Table S13. Selected bond lengths [Å] and angles [°] for **8**.

Mo(1)-O(1)	1.642(2)
Mo(1)-O(2)	1.981(2)
Mo(1)-O(3)	2.012(2)
Mo(1)-O(11)	2.0413(12)
Mo(1)-O(21)	2.0262(12)
Mo(1)-N(1)	2.1810(15)
Mo(1)-N(2)	2.1852(15)
O(2)-O(3)	1.430(3)
O(11)-C(11)	1.3192(19)
C(17)-N(1)	1.294(2)
N(1)-C(101)	1.478(2)
O(21)-C(21)	1.323(2)
C(27)-N(2)	1.293(2)
N(2)-C(201)	1.484(2)
N(1)-Mo(1)-N(2)	160.74(5)
O(1)-Mo(1)-O(11)	170.71(9)
O(2)-Mo(1)-O(21)	156.79(7)
O(3)-Mo(1)-O(21)	154.59(7)
C(11)-O(11)-Mo(1)	130.87(10)
C(17)-N(1)-C(101)	116.14(15)
C(17)-N(1)-Mo(1)	123.91(12)
C(101)-N(1)-Mo(1)	119.84(11)
C(21)-O(21)-Mo(1)	131.94(11)
C(27)-N(2)-C(201)	116.12(15)
C(27)-N(2)-Mo(1)	123.61(11)
C(201)-N(2)-Mo(1)	120.22(11)

Crystal structure determination of 9. All the measurements were performed using monochromatized Mo K_α radiation at 100K: $C_{42}H_{52}MoN_2O_5 \cdot C_2H_3N$, M_r 801.85, triclinic, space group P -1, a = 11.644(3)Å, b = 13.947(3)Å, c = 14.644(4)Å, α = 107.150(5)°, β = 104.487(6)°, γ = 98.883(6)°, V = 2132.3(9)$Å^3$, Z = 2, d_{calc} = 1.249g cm^{-3}, μ = 0.353mm^{-1}. A total of 57870 reflections were collected (Θ_{max} = 30.0°), from which 12427 were unique (R_{int} = 0.0568), with 10530 having $I > 2\sigma(I)$. The structure was solved by direct methods (SHELXS-97)[1] and refined by full-matrix least-squares techniques against F^2 (SHELXL-2014/6).[1] The acetonitrile solvent molecule (N51 to C58) was disordered over four orientations and was refined with site occupation factors of 0.315(3), 0.296(3), 0.295(3), and 0.094(2), resp., summing up to unity. The equivalent bonds in these solvent molecules were restrained to have the same lengths and the same anisotropic displacement parameters were used for closely spaced molecular orientations of this solvent molecule. Consequently, one of the nearby situated *tert.* butyl groups (bonded to C14) and the phenyl ring bonded to N2 also were disordered over two orientations and were refined with site occupation factors of 0.906(2), and 0.094(2), respectively. The C–C bonds in the disordered *tert.* butyl group in the less occupied orientation were restrained to 1.53Å. The C atoms of the disordered phenyl ring in the less occupied orientation were fitted to a regular hexagon with C–C distances of 1.39Å. The same anisotropic displacement parameters were used for equivalent C atoms in these two disordered groups. The other non-hydrogen atoms were refined with anisotropic displacement parameters without any constraints. The H atoms of the phenyl rings and of the imino groups were put at the external bisectors of the X–C–C angles at C–H distances of 0.95Å and common isotropic displacement parameters were refined for the H atoms of the same ring including the H atom of the adjacent imino group. The H atoms of the *tert.* butyl groups and of the methyl groups of the solvent molecules were refined with common isotropic displacement parameters for the H atoms of the same group and idealized geometries with tetrahedral angles, enabling rotation around the C–C bond, and C–H distances of 0.98Å. The H atoms of the disordered *tert*-butyl group in the less occupied orientation were refined with staggered conformations. For 546 parameters final *R* indices of R1 = 0.0368 and wR^2 = 0.0855 (GOF = 1.044) were obtained. The largest peak in a difference Fourier map was 0.755eÅ^{-3}.

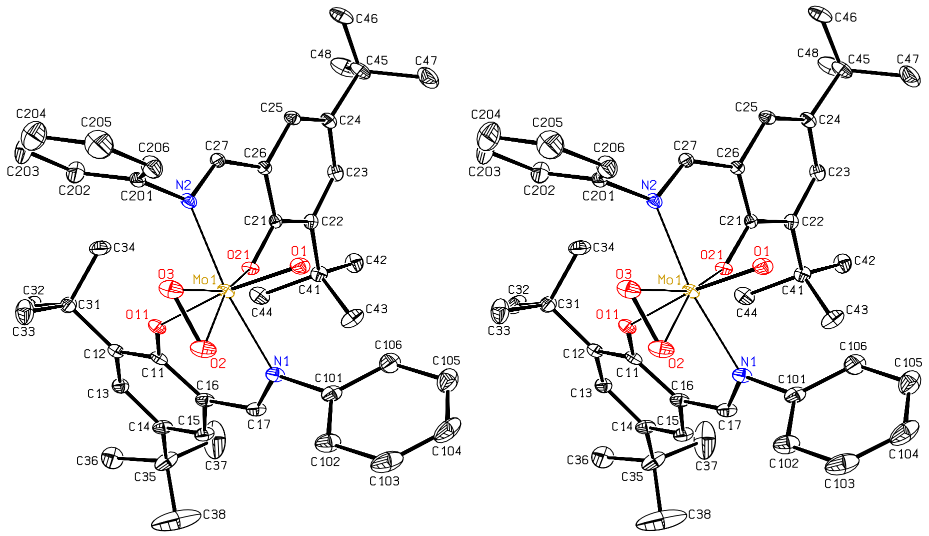

Figure S54. Stereoscopic ORTEP[2] plot of **9** showing the atomic numbering scheme. The probability ellipsoids are drawn at the 50% probability level. The H atoms, the disordered parts of the complex in the orientations with low site occupation factors of 0.094(2), and the disordered acetonitrile solvent molecule were omitted for clarity reasons.

Table S14. Additional crystal data and structure refinement for **9**.

Crystal data	
Calculated density	1.249Mg/m^3
F(000)	844
Linear absorption coefficient μ	0.353mm^{-1}
Absorption correction	semi–empirical from equivalents
Max. and min. transmission	1.000 and 0.723

Data collection	
Temperature	100K
Diffractometer	Bruker APEX–II CCD
Radiation source	Incoatec microfocus sealed tube
Radiation and wavelength	MoK_{α}, 0.71073Å
Monochromator	multilayer monochromator
Scan type	ϕ and ω scans
Refinement	
Refinement method	Full–matrix least–squares on F^2
Extinction expression	none
Structure Solution Program	SHELXS–97 (Sheldrick, 2008)
Structure Refinement Program	SHELXL–2014/6 (Sheldrick, 2008)

Table S15. Selected bond lengths [Å] and angles [°] for **9**.

Mo(1)-O(1)	1.6928(13)
Mo(1)-O(2)	1.9581(13)
Mo(1)-O(3)	1.9301(13)
Mo(1)-O(11)	2.0166(12)
Mo(1)-O(21)	2.0493(12)
Mo(1)-N(1)	2.2137(15)
Mo(1)-N(2)	2.1654(15)
O(2)-O(3)	1.4425(18)
O(11)-C(11)	1.3289(19)
C(17)-N(1)	1.296(2)
O(21)-C(21)	1.320(2)
C(27)-N(2)	1.301(2)
O(1)-Mo(1)-O(11)	162.17(5)
O(2)-Mo(1)-O(21)	155.35(5)
O(3)-Mo(1)-O(21)	155.32(5)
N(1)-Mo(1)-N(2)	164.52(5)
C(11)-O(11)-Mo(1)	133.31(11)
C(17)-N(1)-C(101)	116.92(15)
C(17)-N(1)-Mo(1)	125.59(12)
C(101)-N(1)-Mo(1)	117.32(10)
C(21)-O(21)-Mo(1)	128.53(10)
C(27)-N(2)-C(201)	115.49(15)
C(27)-N(2)-Mo(1)	121.54(12)
C(201)-N(2)-Mo(1)	121.57(12)

References

1 G. M. Sheldrick, *Acta Crystallogr., A*, 2008, **64**, 112–122.
2 C. K. Johnson, *ORTEP. Report ORNL-3794.*, Tennessee, USA, 1965.